Dynamics of Interdecadal Variability in Coupled Ocean–Atmosphere Models

M. LATIF

Max-Planck-Institut für Meteorologie, Hamburg, Germany

(Manuscript received 18 February 1997, in final form 17 July 1997)

ABSTRACT

The interdecadal variability as simulated by coupled ocean–atmosphere models is reviewed. Emphasis is given to that class of interdecadal variability that arises from ocean–atmosphere interactions. The interdecadal variability simulated can be classified roughly into four classes: tropical interdecadal variability, interdecadal variability that involves both the Tropics and the extratropics as active regions, midlatitudinal interdecadal variability involving the wind-driven ocean gyres, and midlatitudinal interdecadal variability involving the thermohaline circulation. Several coupled models predict the existence of different interdecadal climate cycles, with periods ranging from approximately 10–50 yr. This implies some inherent predictability at decadal timescales, provided that these interdecadal cycles exist in the real climate system.

1. Introduction

The causes of interdecadal climate variability can be quite different, including external and internal forcing mechanisms. On the one hand, external forcing mechanisms have been discussed for a long time. Variations in the incoming solar radiation, for instance, were proposed as one of the major sources of interdecadal variability (e.g., Labitzke 1987; Lean et al. 1995). Cubasch et al. (1997) show indeed that some climate impact of the sun might exist on timescales of many decades and longer, but it is fairly controversial at present how strong the fluctuations in the solar insolation actually are. The forcing of interdecadal climate variability by volcanos is well established and therefore less controversial, and major volcanic eruptions can be easily seen in regional and globally averaged temperature records (e.g., Robock and Mao 1995).

On the other hand, interdecadal variability arises from interactions within and between the different climate subsystems. The two most important climate subsystems are the ocean and the atmosphere. Nonlinear interactions between different space and timescales can produce interdecadal variability in both the ocean (e.g., Jiang et al. 1995; Spall 1996) and the atmosphere (e.g., James and James 1989) as shown by many modeling studies. More important, however, seem to be the interactions between the two systems. The stochastic climate model scenario proposed by Hasselmann (1976) is a ''one-way'' interaction: the atmospheric ''noise'' (the high-frequency weather fluctuations) drives low-frequency changes in the ocean, leading to a red spectrum in the ocean's sea surface temperature (SST), for instance, in analogy to Brownian motion. It has been shown that the interannual variability in the midlatitudinal upper oceans is consistent with Hasselmann's (1976) stochastic climate model (e.g., Frankignoul and Hasselmann 1977). This concept has been generalized recently by Frankignoul et al. (1997), who incorporated the wind-driven ocean gyres into the stochastic climate model concept, which extends the applicability of the stochastic climate model to interdecadal timescales. The atmospheric noise can also excite damped eigenmodes of the ocean circulation on interdecadal to centennial timescales, as shown, for instance, by the model studies of Mikolajewicz and Maier-Reimer (1990), Weisse et al. (1994), and Griffies and Tziperman (1995).

''Two-way'' interactions between the ocean and the atmosphere in the form of unstable ocean–atmosphere interactions were also proposed to cause interdecadal climate variability (e.g., Latif and Barnett 1994; Gu and Philander 1997; Chang et al. 1997). Similar to the El Niño–Southern Oscillation (ENSO) phenomenon (e.g., Philander 1990; Neelin et al. 1994), ocean and atmosphere reinforce each other, so that perturbations can grow to climatological importance. The memory of the coupled system (which resides generally in the ocean) provides delayed negative feedbacks, which enable continuous, but probably damped, oscillations that are forced by the internal noise within the coupled ocean–atmosphere system.

The intention behind this review paper is to summarize the mechanisms that lead to interdecadal variability in coupled ocean–atmosphere models. The prob-

Corresponding author address: Dr. Mojib Latif, Max-Planck-Institut für Meteorologie, Bundesstrasse 55, D-20146 Hamburg, Germany.
E-mail: latif@dkrz.de

lem of interdecadal variability is approached by using a hierarchy of coupled models. Some mechanisms were investigated with relatively complex coupled models in which at least one component is represented by a general circulation model (GCM) (e.g., Delworth et al. 1993; Latif and Barnett 1994; Grötzner et al. 1998; Saravanan and McWilliams 1997; Chen and Ghil 1996; Xu et al. 1998), while other mechanisms were studied using relatively simple or conceptual models (e.g., Gu and Philander 1997; Chang et al. 1997). It should be noted that this paper does not attempt to provide a complete overview of all mechanisms that can lead to interdecadal variability. Emphasis is given to those modes that were either identified in coupled ocean–atmosphere models, or for which ocean–atmosphere interactions are crucial. Several ''ocean-only'' modes (e.g., Weaver and Sarachik 1991; Weaver et al. 1993; Weisse et al. 1994; Jacobs et al. 1994), for instance, identified in uncoupled ocean model simulations are not described here. Sensitivity studies with coupled models (e.g., Meehl 1996) are also not described in this review article.

Furthermore, this paper does not aim to provide a complete overview of the observational work documenting interdecadal variability. Observations are presented only to motivate some of the modeling studies and to verify some of the modeling results. The reader is referred to the observational papers of, for example, Folland et al. (1986), Dickson et al. (1988), Mysak et al. (1990), Deser and Blackmon (1993), Kushnir (1994), Trenberth and Hurrell (1994), Mann and Park (1994), Levitus and Antonov (1995), Zhang et al. (1997), Mantua et al. (1997), and references therein for further information on the observational aspects of interdecadal variability. A fairly comprehensive overview of the different aspects of interdecadal variability (including theoretical, modeling, and observational studies) can be found in the recent book published by Anderson and Willebrand (1996).

The paper is organized as follows. The interdecadal variability that originates in the Tropics is described in section 2. Interactions between the Tropics and midlatitudes that may lead to interdecadal variability are discussed in section 3. The interdecadal variability, which is associated with the midlatitudinal ocean gyres, is described in section 4, while the interdecadal variability, which arises from variations in the thermohaline circulation, is summarized in section 5. A brief overview of studies dealing with the predictability at decadal timescales is given in section 6. The paper is concluded with a discussion in section 7.

2. Interdecadal variability originating in the Tropics

a. The tropical Pacific

The tropical Pacific Ocean has a prominent role in forcing global climate anomalies. This is due to the existence of the El Niño–Southern Oscillation (ENSO) phenomenon, the strongest interannual climate fluctuation (see, e.g., Philander 1990). It is likely that interdecadal fluctuations in tropical Pacific SST will also have a significant impact on regional and global climate. Interdecadal northeastern Australian rainfall anomalies, for instance, were shown to be highly correlated with interdecadal fluctuations in tropical Pacific SST (Latif et al. 1997a).

ENSO is a classic example of an inherently coupled air–sea mode, which is characterized by a dominant period of about 4 yr. The spectrum of tropical Pacific SST, however, is relatively broad due to the presence of noise and/or nonlinear interactions between the annual cycle and the dominant ENSO mode. Here, results are shown from the study of Eckert and Latif (1997), who investigated the role of the stochastic forcing on the low-frequency variability in the tropical Pacific.

A series of experiments were performed with a hybrid coupled model (HCM), consisting of an oceanic general circulation model (OGCM) and a statistical atmosphere model. The latter is an equilibrium atmosphere (see, e.g., Barnett et al. 1993), which does not simulate any internal variability. The HCM simulates self-sustained oscillations with a period of about 5 yr at sufficiently strong coupling (Fig. 1a). The spectrum of the simulated SST anomalies, however, is unrealistic when compared to that derived from the SST observations, with one relatively strong and narrow peak at the dominant ENSO frequency (Fig. 1d). The inclusion of stochastic forcing leads to a much more realistic simulation (Fig. 1b), and the spectrum of the simulated SST anomalies is now in better agreement with the spectrum of the observed SST anomalies. In particular, the stochastically forced HCM simulates considerable interdecadal variability. As can be inferred from the experiment with the uncoupled ocean model (zero coupling strength) forced by noise only (Fig. 1c), the level of the simulated interdecadal variability is much lower relative to the coupled case. Thus, the coupling between ocean and atmosphere is important in generating not only ENSO itself but also some part of the interdecadal variability in the tropical Pacific by amplifying the noise in the system. However, the level of the interdecadal variability simulated in the coupled integration with noise is lower than that observed, indicating that other processes such as the nonlinear interactions between different timescales or interactions with phenomena outside the tropical Pacific may be also important in generating interdecadal variability in the tropical Pacific (see also section 3).

Similar results are obtained from the Lamont intermediate coupled model (ICM), described in detail by Zebiak and Cane (1987), which is also a regional model of the tropical Pacific. The Lamont model simulates not only considerable interdecadal but also centennial variability (Fig. 2). Since the atmospheric component of the Lamont model generates internal variability, it is likely that the occurrence of the low-frequency variability is

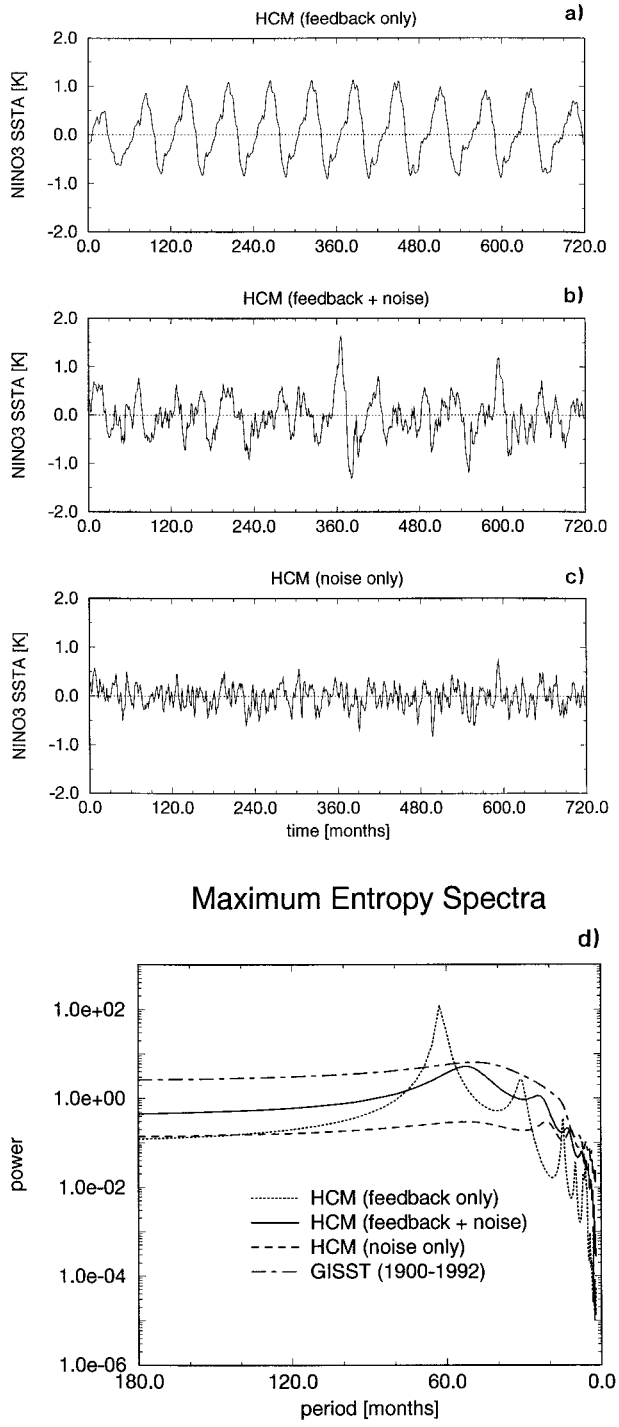

FIG. 1. Time series and spectra of SST anomalies (°C) averaged over the Niño-3 region (150°–90°W, 5°N–5°S) as simulated by the Eckert and Latif (1997) HCM. (a) Niño-3 SST anomaly time series simulated in the unperturbed coupled control integration; (b) Niño-3 SST anomaly time series simulated in the coupled integration with noise; (c) Niño-3 SST anomaly time series simulated in the integration without atmospheric feedback (uncoupled ocean model) but with noise included. (d) Spectra of the time series shown in Figs. 1a–c. The spectrum of the observed Niño-3 SST anomaly as derived from the GISST dataset of the British Meteorological Office is shown for comparison.

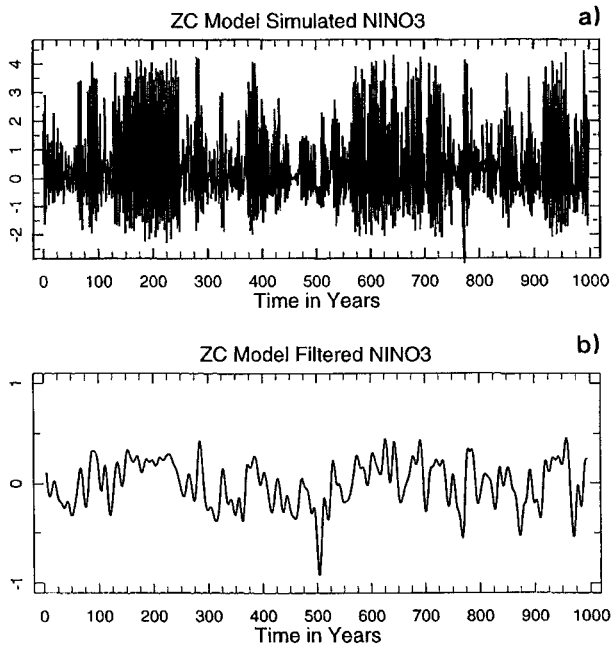

FIG. 2. Niño-3 SST anomalies (°C) as simulated by the Zebiak and Cane (1987) ICM in a 1000-yr control integration. (a) Raw time series based on monthly values; (b) low-pass filtered Niño-3 SST anomaly time series in which variability with timescales longer than approximately 10 yr is retained.

also related, at least partly, to the stochastic forcing, as described above. Nonlinear effects, however, might be also important (e.g., Münnich et al. 1991; Jin et al. 1994). In summary, coupled processes within the tropical Pacific climate system can produce considerable interdecadal variability, which will have global climate impacts through atmospheric teleconnections (e.g., Horel and Wallace 1981; Glantz et al. 1991).

b. The tropical Atlantic

Interdecadal variability in the tropical Atlantic evolves rather differently than that in the tropical Pacific, which is probably due to the different basin geometries. While the zonal wind stress/SST feedback is the dominant growth mechanism in the equatorial Pacific and the surface heat flux acts as a damping, the surface heat flux has a much more active role in the tropical Atlantic [see Chang et al. (1997) for a good summary and references therein]. A weak ENSO-like mode, however, exists also in the equatorial Atlantic (e.g., Zebiak 1993; Carton and Huang 1994), with a timescale of about 2.5 yr (Latif et al. 1996a).

The existence of a decadal dipole mode with opposite SST anomalies north and south of the intertropical convergence zone (ITCZ) has been postulated by several authors (e.g., Mehta and Delworth 1995; Chang et al. 1997). The SST dipole influences the rainfall over parts of South America, as shown by Moura and Shukla (1981), and there is some evidence that Sahelian rainfall

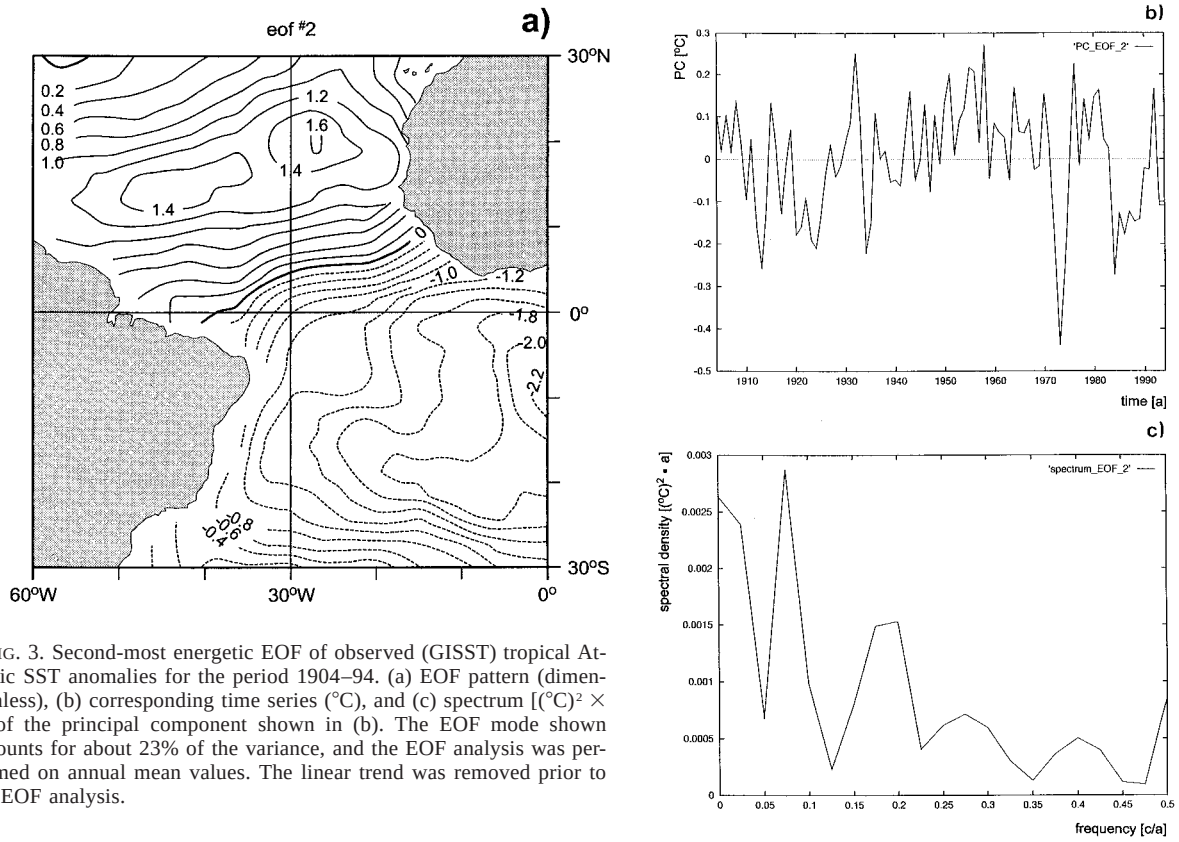

FIG. 3. Second-most energetic EOF of observed (GISST) tropical Atlantic SST anomalies for the period 1904–94. (a) EOF pattern (dimensionless), (b) corresponding time series (°C), and (c) spectrum [(°C)^2 × *a*] of the principal component shown in (b). The EOF mode shown accounts for about 23% of the variance, and the EOF analysis was performed on annual mean values. The linear trend was removed prior to the EOF analysis.

is also affected by the dipole [see, e.g., Lamb and Peppler (1991) for a good overview]. However, it is controversial as to whether there exists a distinct timescale, and even the existence of the dipole structure itself is questioned in some studies (e.g., Houghton and Tourre 1992; Enfield and Mayer 1997; Mehta 1998). Carton et al. (1996), for instance, accept the existence of the spatial dipole structure, but they argue that its dynamics can be described to first order by the stochastic climate model of Hasselmann (1976). Chang et al. (1997) on the other hand regard the SST dipole as a ''true'' oscillatory mode with a period of approximately 12–13 yr.

To get more insight into the nature of the interdecadal variability in the tropical Atlantic, observed (GISST) annual mean SSTs were analyzed for the period 1904–94. An empirical orthogonal function (EOF) analysis was conducted, and the second most energetic EOF mode accounting for about 23% of the variance is associated with the north–south dipole structure (Fig. 3a) discussed above. A spectral analysis of the corresponding principal component (Fig. 3b) shows indeed enhanced variability at a period of approximately 13 yr (Fig. 3c), which supports Chang et al.'s (1997) hypothesis. It should be noted, however, that the EOF mode accounts for a relatively large fraction of the variance in the Southern Hemisphere only. While the local explained variances amount to typically 40% in the southern center of action, they amount to about 20% only in the northern center of action. Furthermore, as will be shown below (section 4b), a mode in the North Atlantic with a period of about 12 yr was identified by Deser and Blackmon (1993). It is unclear to which extent the tropical dipole and the midlatitudinal mode reflect the same phenomenon, or whether and how they interact with each other.

Chang et al. (1997) derived a plausible theory that would explain physically the ''dipole-oscillation'' and its spatial structure by conducting a series of experiments with an ICM and a hybrid coupled model. Here, results are shown from the ICM. The ICM simulates self-sustained interdecadal oscillations for certain parameters, and the simulated spatial structure resembles that observed closely (Fig. 4). The mechanism for the oscillation can be summarized as follows. Suppose the system is in a state similar to that shown in Fig. 4a, with warm SST anomalies north and cold SST anomalies south of the ITCZ. The associated wind response will be such that the trade winds are weakened over the warm SST anomaly in the north and strengthened over the cold SST anomaly in the south. This will lead to surface heat flux anomalies that reinforce the initial SST anomalies in both poles of the dipole. Thus, the air–sea interactions over the tropical Atlantic are unstable. The horizontal advection of heat by the steady ocean currents

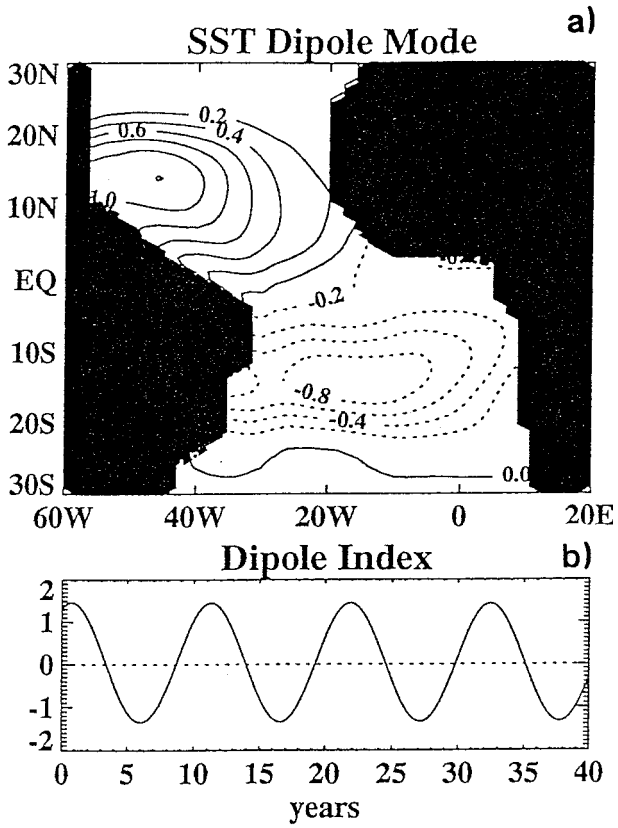

FIG. 4. The tropical Atlantic dipole mode as simulated by the ICM of Chang et al. (1996). Shown is (a) the characteristic SST anomaly pattern as obtained from a regression analysis of the SST anomalies upon a dipole index, which is shown in (b). The dipole index is defined as the difference of the SST anomalies in the two centers of action. See Chang et al. (1997) for details.

will counteract the growth in SST by transporting anomalously cold (warm) water to the north (south). As pointed out by Chang et al. (1997), the system gives rise to self-sustained oscillations when the positive and negative feedbacks balance properly. In this scenario, the Atlantic dipole is an inherently coupled air–sea mode, which might be predictable several years ahead. Preliminary results from decadal forecast experiments with a simplified (hybrid) coupled ocean–atmosphere model support this picture (P. Chang 1996, personal communication).

In summary, unstable air–sea interactions can produce interdecadal variability in both the tropical Pacific and Atlantic Oceans. The characters of the interdecadal variabilities, however, are quite different in the two oceans. While the interdecadal variability in the Pacific is dominated by zonal asymmetries, the interdecadal variability in the Atlantic is dominated by meridional asymmetries. Furthermore, while the dynamical feedback between the zonal wind stress and SST is crucial in the Pacific, it is the thermodynamic feedback between the surface heat flux and SST, which is important to the growth of anomalous conditions in the Atlantic.

3. Tropics–midlatitudes interactions

A hypothesis for the generation of interdecadal variability based on Tropics–midlatitudes interactions was proposed by Gu and Philander (1997). Their theory is based on the existence of a shallow meridional circulation, which links the Tropics to the extratropics. Certain pathways were identified in the ocean through which information can flow from the extratropics toward the Tropics (e.g., Liu et al. 1994; Liu and Philander 1995; Lu and McCreary 1995). These pathways, which are mainly located in the central and eastern Pacific, are given by surfaces of constant densities (isopycnals). Temperature anomalies at the surface in the extratropics can affect the Tropics by traveling along the ispoycnals into the equatorial thermocline, where the anomalies are upwelled to the surface. Unstable air–sea interactions will further amplify the signal.

Suppose a warm interdecadal SST anomaly exists in the equatorial Pacific (Fig. 5a). The local and remote atmospheric responses to this SST anomaly will be similar to those observed during El Niño situations, that is, westerly wind anomalies over the western equatorial Pacific and strengthened westerlies in midlatitudes (Fig. 5b). The intensified westerlies will force a negative SST anomaly in the North Pacific, mostly through enhanced heat loss from the ocean to the atmosphere. The cold anomaly will be subducted and flow equatorward along isopycnals. Once it has reached the equatorial region, it will be upwelled to the surface and the SST tendency will be reversed. Gu and Philander (1997) show by means of a simple box model that their subduction mechanism can lead to continuous interdecadal oscillations with a period of the order of several decades. Observational evidence for Gu and Philander's (1997) theory is provided by the work of Deser et al. (1996), who investigated the evolution of the subsurface temperatures in the Pacific for the period 1970–91. Deser et al. (1996) show that a negative temperature anomaly propagated slowly equatorward along isopycnals during the period analyzed (Fig. 6).

The theory of Gu and Philander might explain the interdecadal variability observed in the ENSO activity and predictability (e.g., Balmaseda et al. 1995). The ENSO cycle was not well developed, for instance, during the 1990s (e.g., Goddard and Graham 1997; Ji et al. 1996; Latif et al. 1997a), and most ENSO prediction models failed to forecast correctly the evolution of tropical Pacific SSTs during this period (e.g., Latif et al. 1998). It is well known from ENSO theory (Zebiak and Cane 1987; Neelin et al. 1994) that the instability characteristics depend on the position of the equatorial thermocline. A deeper thermocline, for instance, might inhibit the coupled system to oscillate, and this might have been the case during the 1990s. The theory of Gu and Philander (1997), however, still needs to be proven by means of more complex coupled ocean–atmosphere models.

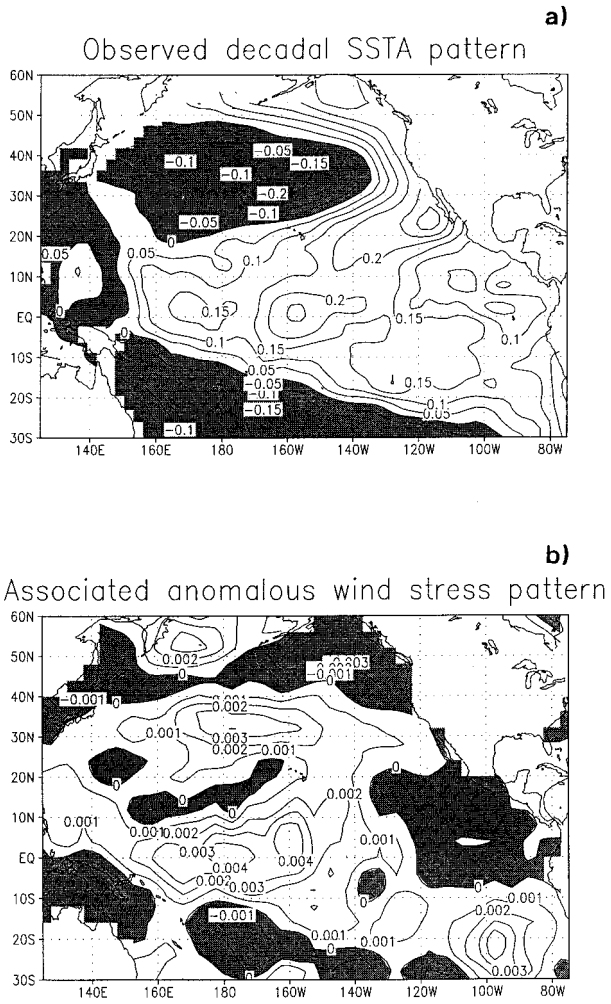

FIG. 5. (a) Spatial pattern of the leading EOF mode of low-pass filtered (retaining variability with timescales longer than 5 yr) observed (GISST) SST anomalies in the Pacific for the period 1949–90. The EOF mode accounts for 44% of the variance. (b) Associated regression pattern of observed (da Silva et al. 1994) zonal wind stress anomalies (N m^{-2}) to the principal component of the leading EOF mode. Shaded areas denote negative values in both panels.

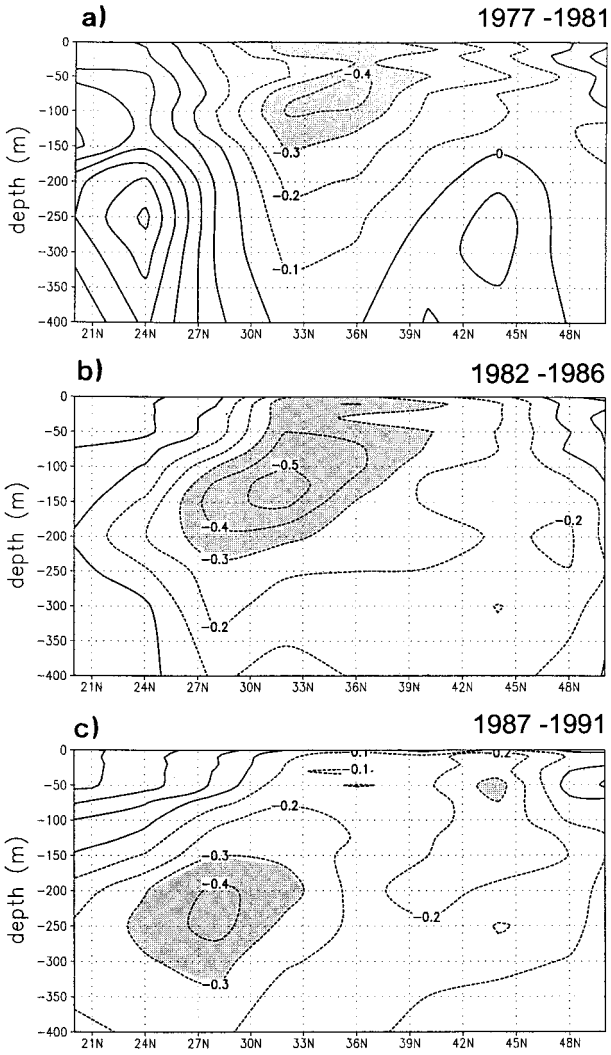

FIG. 6. Anomalies of zonally averaged (170°–145°W) temperature (°C) as function of depth and latitude in the Pacific for different time periods: (a) 1977–81, (b) 1982–86, (c) 1987–91. Anomalies of less than −0.3°C are shaded. As shown by Deser et al. (1996), the negative temperature anomalies spread along isopycnals. See Deser et al. (1996) for details.

4. Midlatitudinal decadal variability involving the wind-driven gyres

A mechanism for interdecadal climate variability that can lead to interdecadal climate cycles in the North Pacific and North Atlantic Oceans was proposed by Latif and Barnett (1994), Latif and Barnett (1996), Latif et al. (1996b), and Grötzner et al. (1998) by analyzing the results of a multidecadal integration with the coupled ocean–atmosphere general circulation model ECHO-1 described by Latif et al. (1994). Similar results were obtained by Robertson (1996) for the North Pacific and Zorita and Frankignoul (1997) for the North Atlantic, who investigated the interdecadal variability simulated in the ECHAM1/LSG CGCM described by von Storch (1994). The interdecadal modes derived from the ECHAM1/LSG coupled model, however, are much more damped relative to those simulated by the ECHO-1 coupled model. The same seems to be true for the modes identified in the Geophysical Fluid Dynamics Laboratory (GFDL) coupled model described by Manabe and Stouffer (1996). There is gyre-related interdecadal variability in the GFDL coupled model, but it differs (like the ECHAM1/LSG model) from that simulated by the ECHO-1 model, probably due to the differing degrees of air–sea coupling, as discussed below. Pronounced interdecadal variability is also simulated by the Hadley Centre CGCM in the North Pacific and North Atlantic Oceans (Tett et al. 1998), but the mechanisms that lead to the interdecadal variability have not been investigated yet.

The gyre modes are generated by large-scale ocean–atmosphere interactions in midlatitudes and must be regarded as inherently coupled modes, as originally suggested by Bjerknes (1964). The memory of the coupled system, however, resides in the ocean and is associated with slow changes in the subtropical ocean gyres. The existence of such interdecadal cycles provides the basis of long-range climate forecasting at decadal timescales in midlatitues (see section 6). A detailed description of the gyre mechanism can be found in Latif et al. (1996b), who describe a series of coupled and uncoupled numerical experiments and in Weng and Neelin (1998, manuscript submitted to *J. Climate*), who derive analytical prototypes for ocean–atmosphere interactions in midlatitudes.

a. The North Pacific gyre mode

Latif and Barnett (1994) introduced the hypothesis of the interdecadal North Pacific coupled mode. When, for instance, the subtropical ocean gyre is anomalously strong, more warm tropical waters are transported poleward by the western boundary current and its extension, leading to a positive SST anomaly in the North Pacific (Fig. 7). The atmospheric response to this SST anomaly is the Pacific–North American (PNA) pattern, which is associated with changes at the air–sea interface that reinforce the initial SST anomaly, so that ocean and atmosphere act as a positive feedback system. The atmospheric response, however, consists also of a wind stress curl anomaly, which spins down the subtropical ocean gyre, thereby reducing the poleward heat transport and the initial SST anomaly. The ocean adjusts with some time lag to the change in the wind stress curl, and it is this transient ocean response that allows continuous oscillations. The corresponding evolution in upper-ocean heat content in the North Pacific, as derived from the Latif and Barnett (1994) simulation, is shown in Fig. 8. The upper-ocean heat content anomalies as reconstructed from the leading complex EOF (CEOF) mode show a clockwise rotation around the subtropical gyre, which can be partly attributed to baroclinic Rossby wave adjustment and advection of temperature anomalies by the mean gyral circulation. Xu et al. (1997) was able to reproduce the results of Latif and Barnett (1994) with a hybrid coupled model of the North Pacific, confirming that the Tropics play a minor role. As will be shown below, this characteristic evolution of temperature anomalies at subsurface levels can be exploited for the prediction of decadal climate changes (Fig. 21).

Observations support the existence of the interdecadal cycle in the North Pacific–North American climate system. Latif and Barnett (1996), for instance, demonstrate the existence of a 20-yr periodicity by analyzing station data of surface temperature and rainfall over North America since 1860. This is consistent with the study of Haston and Michaelson (1994), who reconstructed Central Californian coastal rainfall for the last 600 yr.

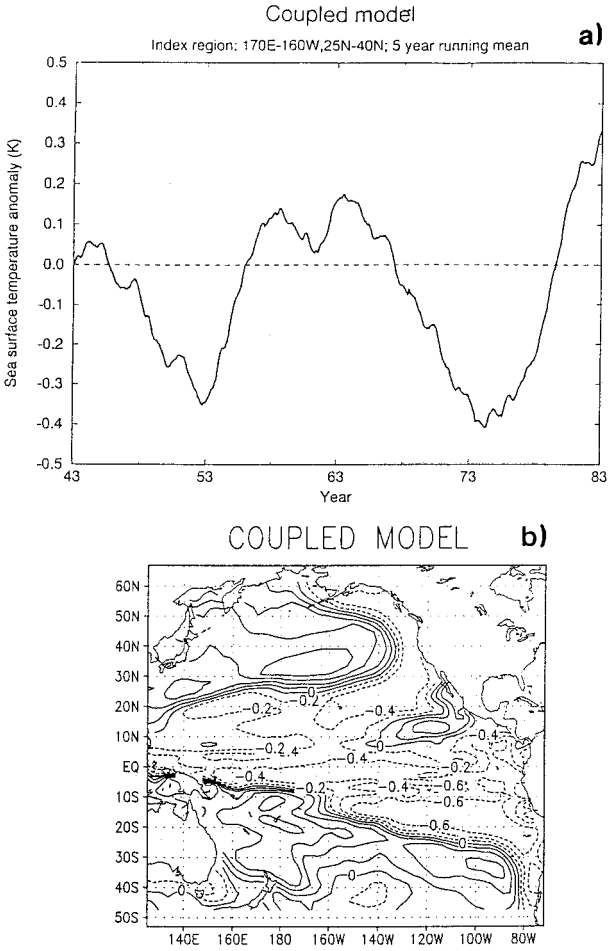

FIG. 7. (a) Low-pass filtered (retaining variability with timescales longer than 5 yr) anomalous sea surface temperature (°C) averaged over the North Pacific (170°E–160°W, 25°–40°N) as simulated by the ECHO-1 CGCM. (b) Spatial distribution of correlation coefficients of the index time series shown in (a) and low-pass filtered SST anomalies in the Pacific. See Latif et al. (1996b) for details.

Robertson (1996) found some evidence of a 30-yr periodicity in North Pacific SST. It should be kept in mind, however, that timescale estimates are subject to large uncertainties due to the relatively short observational records available. Finally, a similar rotation in upper-ocean heat content to that described by Latif and Barnett (1994) was identified by Zhang and Levitus (1997) in the observations (Figs. 9, 10, and 11). They investigated the anomalous three-dimensional temperatures in the North Pacific during the period 1960–90 by means of EOF analysis. The two leading EOF modes of the combined temperature variability show a consistent phase relationship to each other, with EOF mode 2 leading EOF mode 1 by several years (Fig. 9). Thus, the temperature variability reconstructed from the two leading EOFs can be described as a cyclic sequence of patterns (Figs. 10 and 11). In particular, the observations show a clockwise rotation of the subsurface temperature anomalies, similar to that in the ECHO-1 CGCM (Fig. 8).

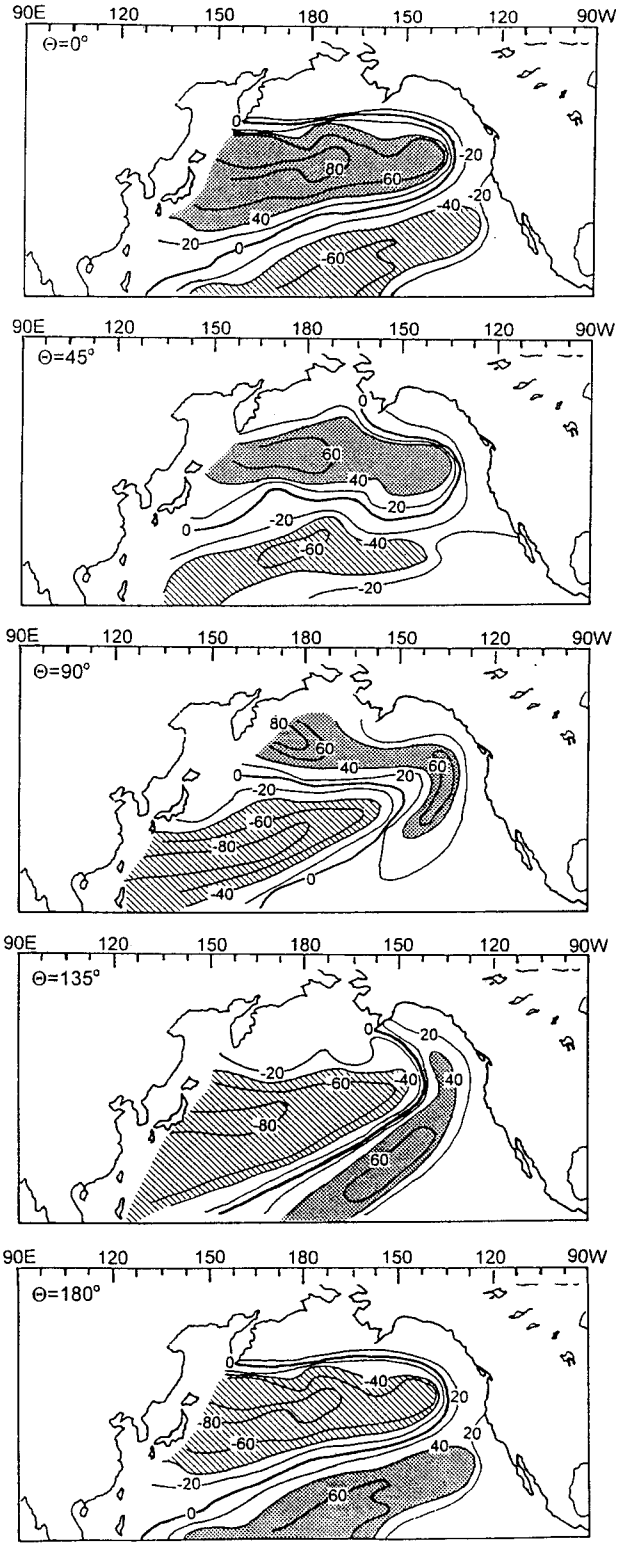

FIG. 8. Evolution of anomalous heat content (°C m) in the ECHO-1 CGCM. The invidual panels show the heat content anomalies at different stages of the decadal cycle, approximately 2.5 yr apart from each other. The heat content anomalies shown are reconstructions from the leading CEOF mode of low-pass filtered (retaining variability with timescales longer than 5 yr) heat content anomalies. See Latif and Barnett (1994) for details.

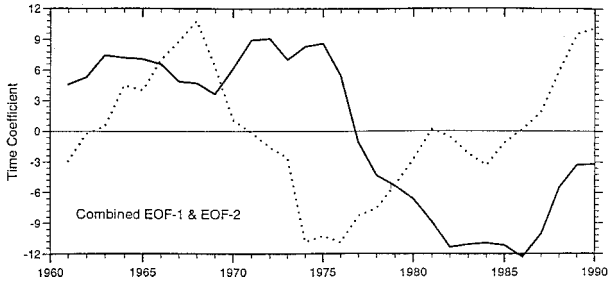

FIG. 9. Time coefficients of the two leading EOFs of the observed low-pass filtered (retaining variability with timescales longer than 3 yr) three-dimensional temperature anomalies in the North Pacific. The first EOF accounting for 27% of the variance is denoted by the solid line, while the second EOF accounting for 17% of the variance is denoted by the dashed line. See Zhang and Levitus (1997) for details.

b. The North Atlantic gyre mode

Similar modes are simulated by some coupled models in the North Atlantic. Zorita and Frankignoul (1997) describe such a mode simulated by the ECHAM1/LSG model, while Grötzner et al. (1998) identified it in the ECHO-1 model. T. Delworth (1996, personal communication) found a weak gyre mode in the GFDL (coarse-resolution) coupled model, which was identified by performing a CEOF analysis of anomalous dynamic height. According to the theory of Latif and Barnett (1994), the period of the North Atlantic gyre mode should be shorter relative to that of the North Pacific gyre mode, and observations support this (e.g., Deser and Blackmon 1993). The characteristic time evolution, SST, and 500-hPa patterns associated with the North Atlantic interdecadal mode as simulated by the Latif et al. (1994) coupled model (ECHO-1) is shown in Fig. 12. The main anomalies are a positive SST anomaly centered near 35°N and a negative SST anomaly to the northwest near 50°N (Fig. 12b). The atmospheric response pattern is reminiscent of the North Atlantic Oscillation (NAO) with centers of action near Iceland and the Azores (Fig. 12c). The evolution in the upper-ocean heat content is very similar to that simulated in the North Pacific (not shown), with a clockwise rotation of the anomalies around the subtropical gyre (Grötzner et al. 1998). The period of the simulated oscillation amounts to about 17 yr in the ECHO-1 model (Fig. 12a), which is longer than observed, while it amounts to about 10 yr in the ECHAM1/LSG model (Zorita and Frankignoul 1997).

Deser and Blackmon (1993) identified an interdecadal mode in the North Atlantic by analyzing surface quantities observed in this century (Fig. 13), and this interdecadal mode shares many aspects of the interdecadal variability simulated in the coupled GCMs investigated by Zorita and Frankignoul (1997) and Grötzner et al. (1998). The spatial surface air temperature anomaly pattern, as expressed by the leading EOF mode, is characterized by a dipole structure (Fig. 13a), and the spectrum (Fig. 13c) of the corresponding principal component (Fig. 13b) shows a statistically significant peak at

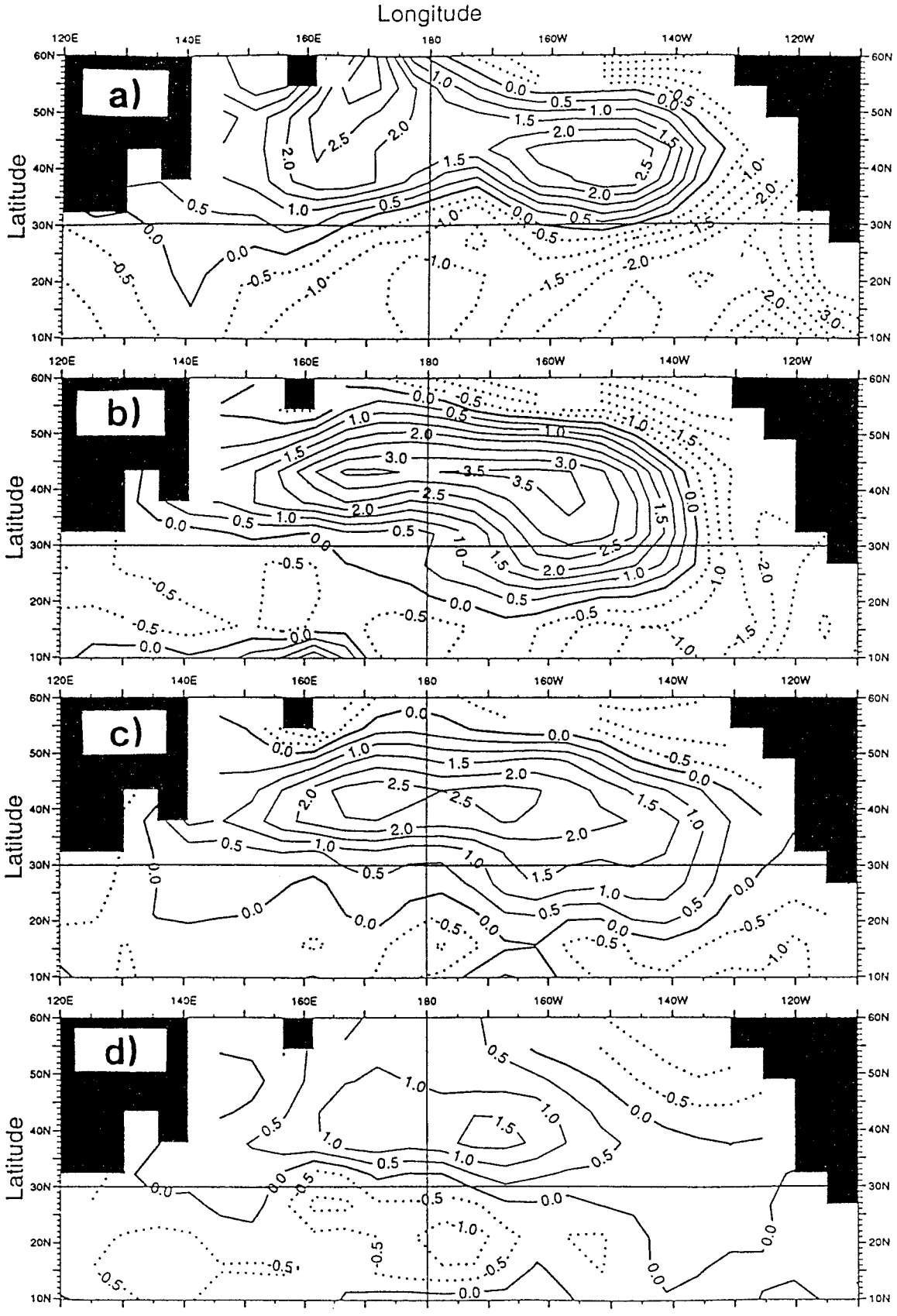
Longitude
120E
140E
160E
180
160W
140W
120W
Latitude
60N
50N
40N
30N
20N
10N
a)
b)
c)
d)

a period of approximaly 12 yr. It should be noted, however, that although a corresponding EOF analysis of the SST anomalies revealed a peak at the same frequency, it was not statistically significant. The atmospheric pressure pattern accompanying the interdecadal surface air fluctuations is very similar to that simulated by the coupled models and reminiscent of the NAO (not shown). Likewise, subsurface temperature anomalies at ocean weather ship C in the North Atlantic at 125-m depth (Levitus et al. 1994) show some remarkable oscillatory behavior during the last few decades, with a period of the order of about 15 yr (Fig. 14). As pointed out by Latif et al. (1996b) and Grötzner et al. (1998), these variations might be forced by the atmosphere in response to variations in the subtropical gyre circulation.

c. *Relative roles of stochastic and deterministic processes*

A competing hypothesis for the generation of interdecadal variability was offered by Frankignoul et al. (1997). They extended the stochastic climate model theory of Hasselmann (1976) to include the variations in the wind-driven ocean gyres. While the coupled interactions proposed by Latif and Barnett (1994) will be associated with a preferred period, the scenario of Frankignoul et al. (1997) predicts a red spectrum with a high-frequency ω^{-2} decay that levels off at low frequency. Different coupled models show quite different qualitative behaviors. The GFDL and the ECHAM1/LSG coupled models, for instance, do not exhibit statistically significant peaks in the spectra of the simulated SSTs in the regions of the subtropical gyres in the North Pacific and North Atlantic, while the Max-Planck-Institut für Meteorologie (MPI) coupled model ECHO-1 does exhibit siginificant decadal peaks in both the North Pacific and North Atlantic.

These differences can be understood partly in terms of the different air–sea coupling strengths (Münnich et al. 1998, manuscript submitted to *J. Phys. Oceanogr.*; Neelin and Weng 1998, manuscript submitted to *J. Climate*). To explore this further, Münnich et al. (1998, manuscript submitted to *J. Phys. Oceanogr.*) coupled a shallow water ocean model to a simple atmospheric feedback. Münnich et al. (1998, manuscript submitted to *J. Phys. Oceanogr.*) investigated three cases. The simple coupled model simulates a damped interdecadal oscillation in the control case (Fig. 15, upper panel). When noise is added to the coupled model, a well-defined spectral peak is retained in the simulation that is superimposed on a red background (Fig. 15, lower panel). This situation corresponds probably to the MPI (ECHO-1) model. When the noise-forced integration is repeated, but with the coupling between ocean and atmosphere turned off, the spectrum of the simulated thermocline depth anomalies is basically red and very close to that predicted by Frankignoul et al.'s (1997) theory (Fig. 15, middle panel). The GFDL and ECHAM1/LSG coupled models reside probably in this latter parameter regime.

Thus, a critical factor determining the character of the interdecadal variability in midlatitudes is the sensistivity of the atmosphere to midlatitudinal SST anomalies. This issue is still a matter of intense scientific discussion. There are, however, some indications that the resolution of the atmosphere model needs to be sufficiently high, in order to represent the atmospheric response adequately, which involves changes in the transient activity (e.g., Palmer and Sun 1985). This is supported by a new integration performed at GFDL. When the GFDL coupled model is run at higher resolution (R30), the nature of the interdecadal variability simulated in the North Pacific seems to change relative to the old run (which used a R15 atmosphere model), and the simulated spatial patterns and timescales are in qualitative agreement with that simulated by the MPI-(ECHO-1) model (T. Delworth 1996, personal communication), which employed an atmosphere model with comparable resolution (T42). In summary, fluctuations in the wind-driven ocean gyres are likely to cause interdecadal climate fluctuations in both the North Pacific and North Atlantic Oceans. The importance of the air–sea coupling and relative roles of stochastic and deterministic processes, however, need to be addressed in more detail.

5. Midlatitudinal interdecadal variability involving the thermohaline circulation

One can separate conceptually the oceanic wind driven from the oceanic thermohaline circulation. While the wind-driven circulation is forced by wind stress variations, the thermohaline circulation is forced by density anomalies. In reality, however, both circulations are coupled to each other, especially in the North Atlantic. Modes were described in the last section, which are to first-order ''pure'' gyre modes. In this section, modes are described that involve mainly the thermohaline circulation as an active component. Delworth et al. (1993) analyzed the multicentury integration with the GFDL (coarse resolution) coupled model described by Manabe and Stouffer (1996). The CGCM simulates pronounced interdecadal variability, as can be inferred from the spectra of two indices of simulated North Atlantic SST

←

FIG. 10. Spatial patterns of the leading EOF mode of the observed three-dimensional temperature variability. The individual panels show the loadings at (a) sea surface, (b) 125-m, (c) 250-m, and (d) 400-m depths, respectively. The corresponding EOF time series is shown in Fig. 9. See Zhang and Levitus (1997) for details.

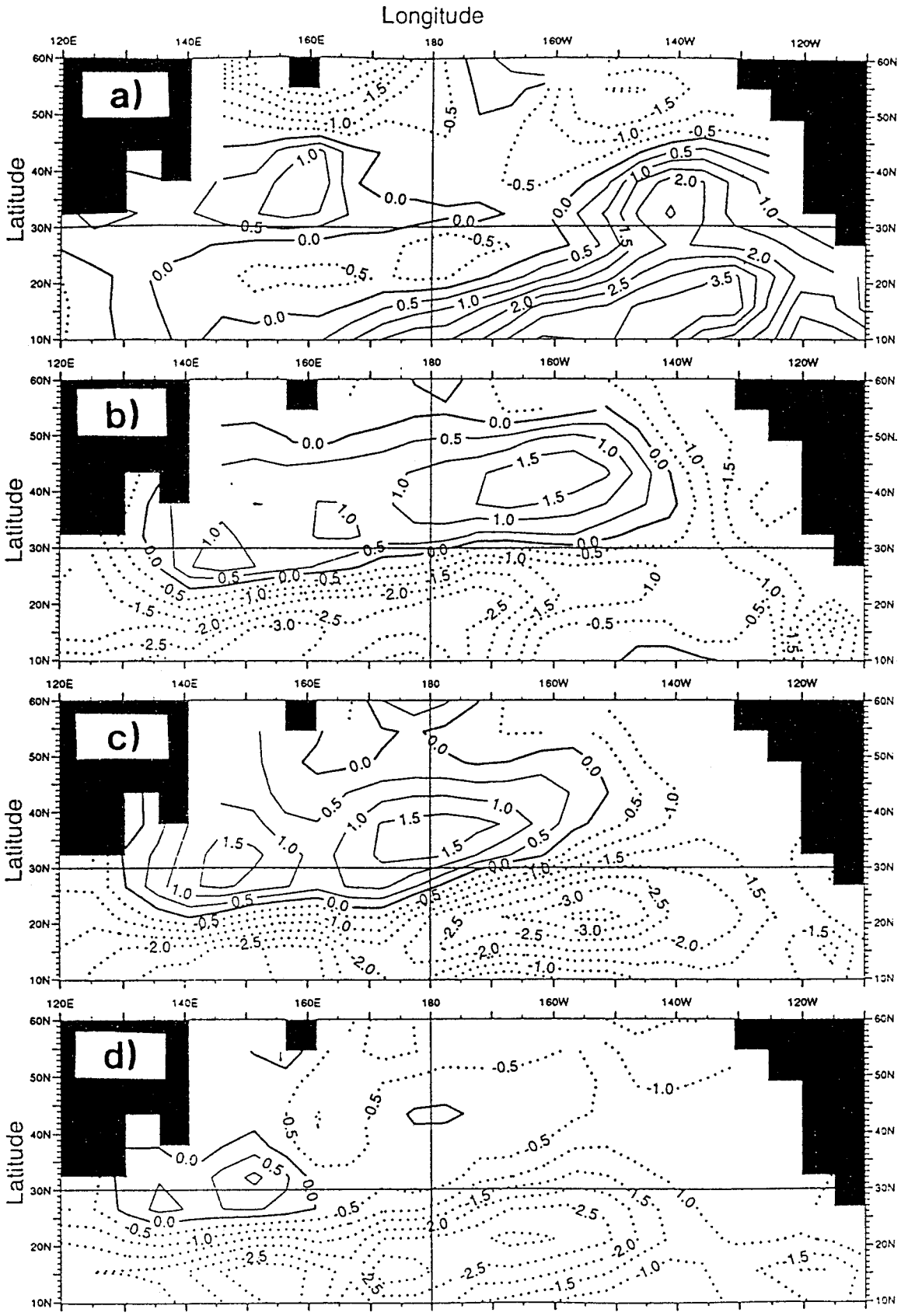
Longitude
120E
140E
160E
180
160W
140W
120W
Latitude
60N
50N
40N
30N
20N
10N
a)
b)
c)
d)

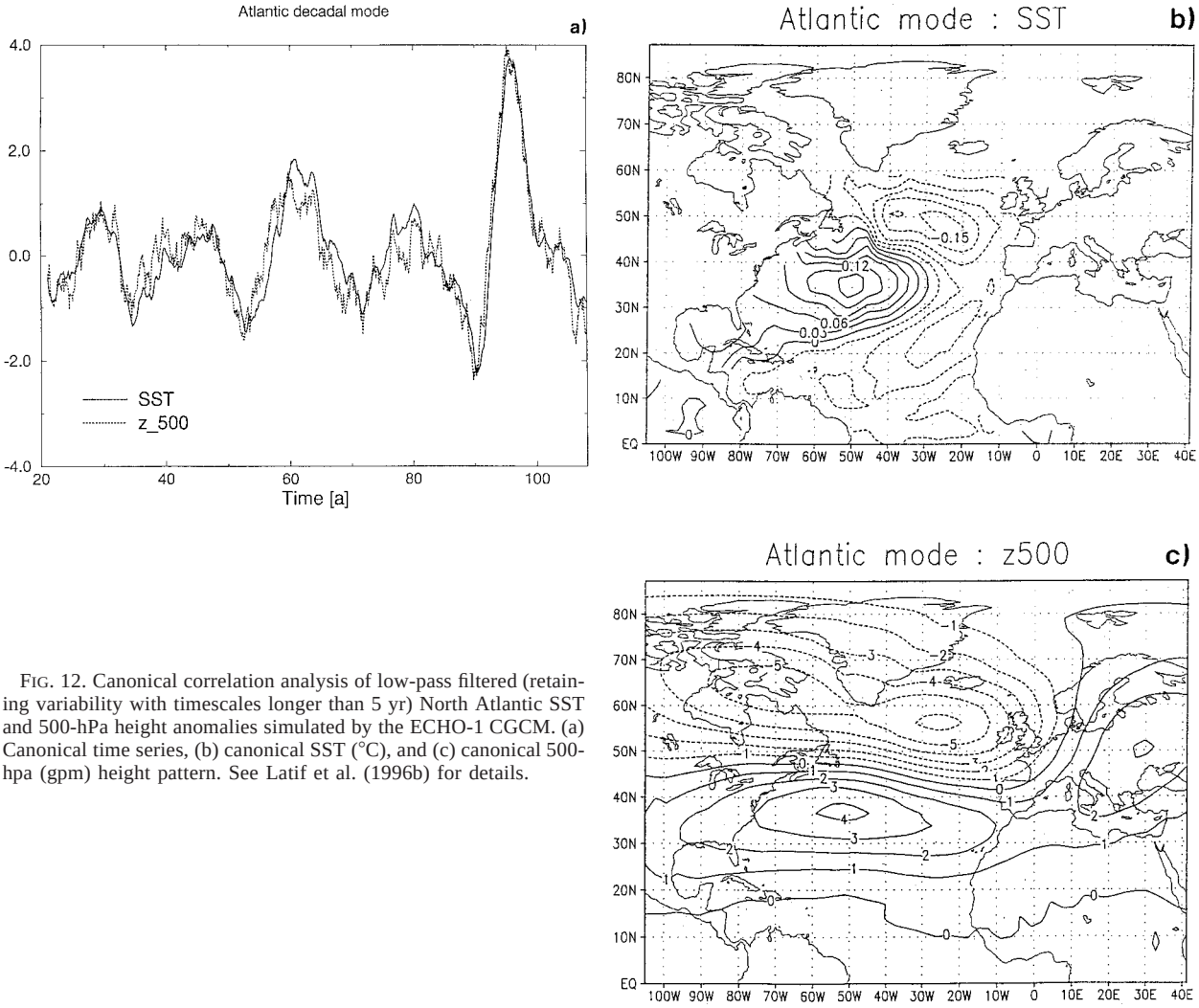

FIG. 12. Canonical correlation analysis of low-pass filtered (retaining variability with timescales longer than 5 yr) North Atlantic SST and 500-hPa height anomalies simulated by the ECHO-1 CGCM. (a) Canonical time series, (b) canonical SST (°C), and (c) canonical 500-hpa (gpm) height pattern. See Latif et al. (1996b) for details.

(Fig. 16a). Enhanced variability is found at 56°N on timescales of several decades, with a spectral peak at a period of 50 yr. Likewise, a meridional overturning index describing the strength of the model's thermohaline circulation (Fig. 16b) shows a similar peak in its spectrum (Fig. 16c). The spatial SST structure of the Delworth et al. (1993) mode agrees favorably with observations described by Kushnir (1994), as shown in Fig. 17.

Delworth et al. (1993) describe their mode basically as an ocean-only mode that does not depend critically on the feedback by the atmosphere. In a later study, Griffies and Tziperman (1995) suggest that the Delworth et al. (1993) mode can be described to first order as a stochastically driven damped linear oscillation. The physics of the mode involves both the thermohaline and a horizontal (gyral) circulation. Salinity-related density anomalies in the sinking region (52°–72°N) drive anomalies in the strength of the thermohaline circulation. The transport of the salinity anomalies into the sinking region is controlled by a horizontal (gyral) circulation, which is mainly controlled by upper-ocean temperature anomalies farther to the south. The gyral circulation, however, is not in phase with the thermohaline circulation, and it is this phase difference between the two circulations that is important to the Delworth et al. (1993) oscillation. The Delworth et al. (1993) mechanism was basically reproduced by Lohmann (1996), who studied the variations of the thermohaline circulation in

←

FIG. 11. Spatial patterns of the secondmost energetic EOF mode of the observed three-dimensional temperature variability. The individual panels show the loadings at (a) sea surface, (b) 125-m, (c) 250-m, and (d) 400-m depths, respectively. The corresponding EOF time series is shown in Fig. 9. See Zhang and Levitus (1997) for details.

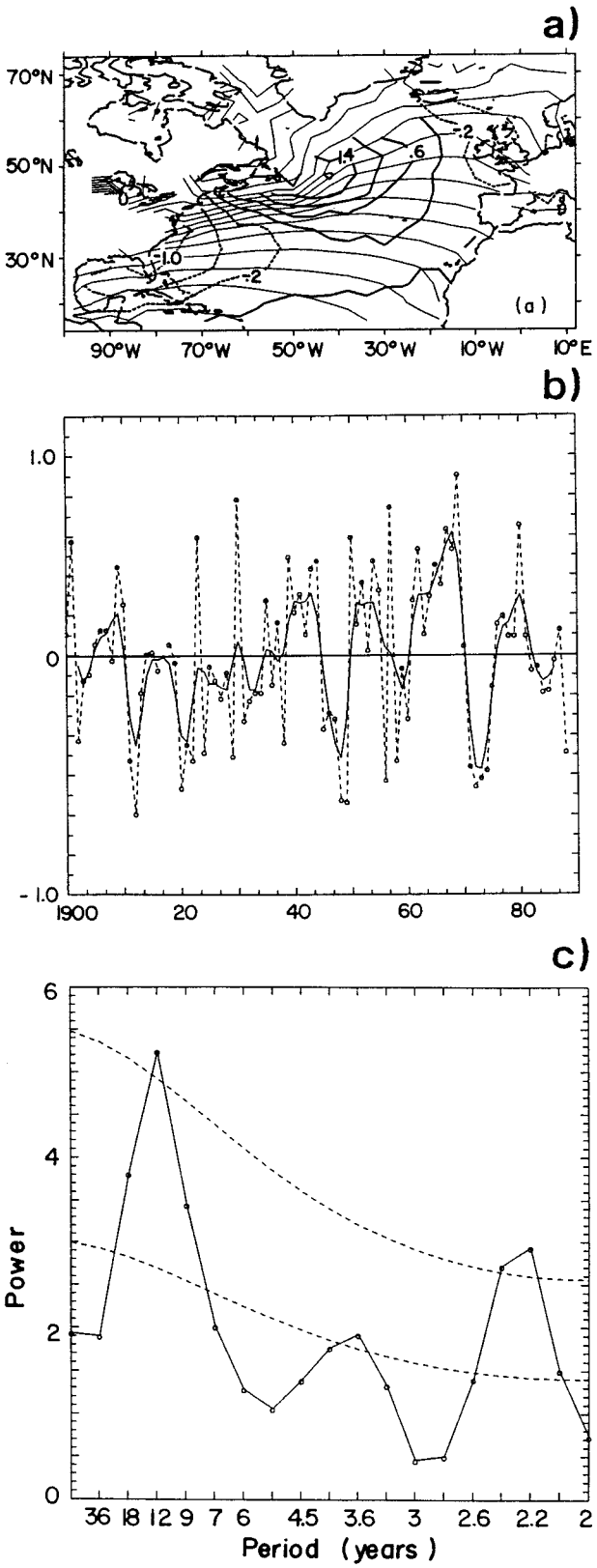

FIG. 13. Leading EOF mode of observed North Atlantic (winter) surface air temperature anomalies. (a) EOF pattern (dimensionless), (b) corresponding principal component (°C), (c) spectrum of the principal component shown in (b). The EOF mode accounts for 21% of the variance. See Deser and Blackmon (1993) for details.

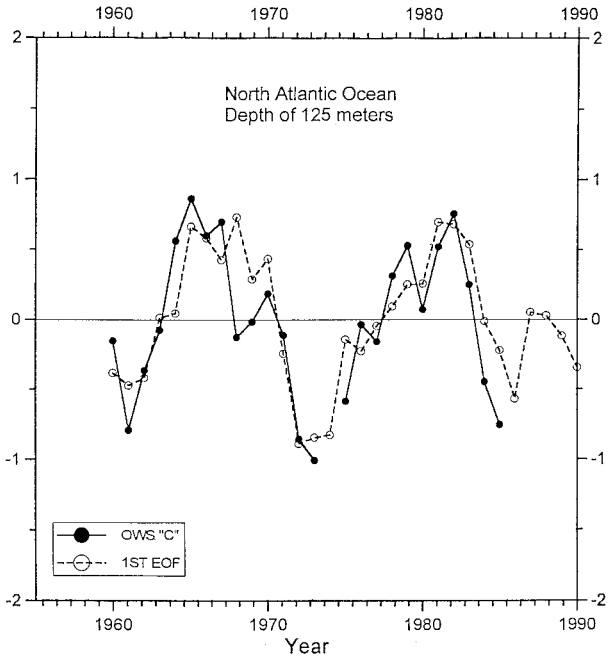

FIG. 14. Time series of subsurface temperature anomalies at 125 m (°C) measured at ocean weather ship "C" (35.5°W, 52.5°N) and time series of the first EOF (multiplied by −1) of North Atlantic temperature anomalies at the same depth. See Levitus et al. (1994) for details.

an OGCM coupled to an energy balance model (EBM). It should be noted that the Delworth et al. (1993) mode seems to be linked to pronounced oscillations in the Greenland Sea (Delworth et al. 1997) and that these oscillations involve the atmosphere as an active component, which has important consequences to the predictability of SST anomalies in the Greenland Sea.

Another interdecadal mode involving the thermohaline circulation was described by Timmermann et al. (1998), who analyzed a multicentury run with the ECHAM3/LSG CGCM. Preliminary results from the first 320 yr of this integration can be found in Latif et al. (1997b). As can be inferred from the overturning index (which was defined in the same way as in Delworth et al. 1993), the coupled model simulates pronounced interdecadal variability, with a statistically significant peak at a period of about 35 yr (Fig. 18). The peak is fairly robust, as was revealed from the full 800 yr of the coupled integration. The level of the interdecadal variability simulated is similar to that in the GFDL (coarse resolution) CGCM. However, in contrast to the Delworth et al. (1993) mode described above, the Timmermann et al. (1998) mode appears to be an inherently coupled ocean–atmosphere mode.

Let us consider the situation 10 yr before the maximum overturning occurs. A well-developed negative SST anomaly covers almost the entire North Atlantic (Fig. 19b) at this time. The atmospheric response as expressed by the anomalous sea level pressure (SLP) is

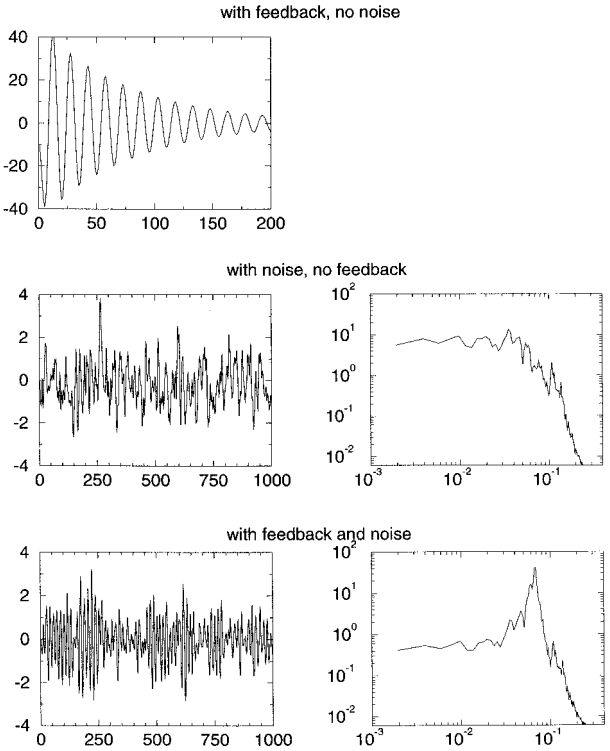

FIG. 15. Interdecadal variability experiments with a simple coupled model. The upper panel shows the thermocline perturbation simulated in a 200-yr control integration, which was perturbed initially. The middle panels show the time series of the thermocline perturbation and the corresponding spectrum obtained in a 1000-yr run without atmospheric feedback but with the inclusion of stochastic forcing. The lower panels show the thermocline perturbation and the corresponding spectrum when both the atmospheric feedback and stochastic forcing are included. See Münnich et al. (1998, manuscript submitted to *J. Phys. Oceanogr.*) for details.

also well developed (Fig. 19a) and is associated with freshwater flux anomalies (not shown) that force positive salinity anomalies off Newfoundland and in the Greenland Sea (Fig. 19c). The convection is near normal at this time (Fig. 19d). The salinity anomalies amplify and propagate into the region of strongest convection, which is located slightly south of Greenland (Fig. 19g), where they strengthen the convection 5 yr later (Fig. 19h). This will eventually lead to an anomalous strong thermohaline circulation, enhanced poleward heat transport in the upper ocean, and the generation of a large-scale positive SST anomaly, which completes the phase reversal. The atmospheric response to this positive SST anomaly will be associated with freshwater flux anomalies, which in turn force negative salinity anomalies off Newfoundland and in the Greenland Sea, opposite to those shown in Fig. 19c, which will eventually initiate the next cold phase. Some elements of this feedback loop were also identified in observations by Wohlleben and Weaver (1995).

The role of the air–sea coupling in generating interdecadal variability associated with the thermohaline circulation is, as in the case of the gyre modes, rather different in the different models. While the Delworth et al. (1993) mode seems to be an ocean-only mode, the Timmermann et al. (1998) mode appears to be an inherently coupled air–sea mode. The differences between the two model simulations may be well explained by the different sensitivities of the respective atmopsheric component models to midlatitudinal SST anomalies. At this stage of understanding, however, we are not in a position to decide which scenario is the more realistic one.

It is interesting to note that salinity anomalies play an important role in both the Delworth et al. (1993) and Timmermann et al. (1998) interdecadal modes. Some simpler coupled models give quite different results. Although similar interdecadal modes are simulated by these simplified models, the temperature effects dominate the salinity effects. The hybrid coupled model of Chen and Ghil (1996), for instance, does not even include salinity effects, while the coupled model of Saravanan and McWillimans (1997) is based on an idealized geometry. These are severe limitations in the formulations of these two particular simplified coupled models. The CGCMs on the other hand employ relatively large flux corrections, especially in the heat and freshwater fluxes. The effects of all these model limitations on the simulation of interdecadal variability are relatively unknown, and much more work is needed in this research area.

6. Predictability at decadal timescales

The problem of the predictability at decadal timescales has two aspects. The first aspect involves the interdecadal variations in the predictability of interannual phenomena, such as ENSO. As shown in a number of studies (e.g., Balmaseda et al. 1995; Chen et al. 1997; Latif et al. 1998; Ji et al. 1996), there is considerable variability in the ENSO prediction skill from decade to decade. The 1970s and the 1990s, for instance, were less predictable than the 1980s, as can be inferred from the ENSO skill scores presented by Chen et al. (1997) (Fig. 20). Some of the interdecadal modes described above may well influence the nature of the ENSO variability and hence the ENSO prediction skill by slowly modulating the background conditions in the tropical Pacific. This issue, however, has not been addressed in great detail so far.

The other aspect of the predictability at decadal timescales involves the prediction of the interdecadal phenomena themselves. S. Venzke (1997, personal communication) investigated the predictability of the North Pacific gyre mode. They forced the ECHAM3 (T42) AGCM by observed SSTs for the period 1949–90 and used the simulated wind stresses and heat fluxes to drive an oceanic GCM. The simulated upper-ocean heat content in the western North Pacific, as expressed by the simulated sea level, shows a remarkable lead–lag re-

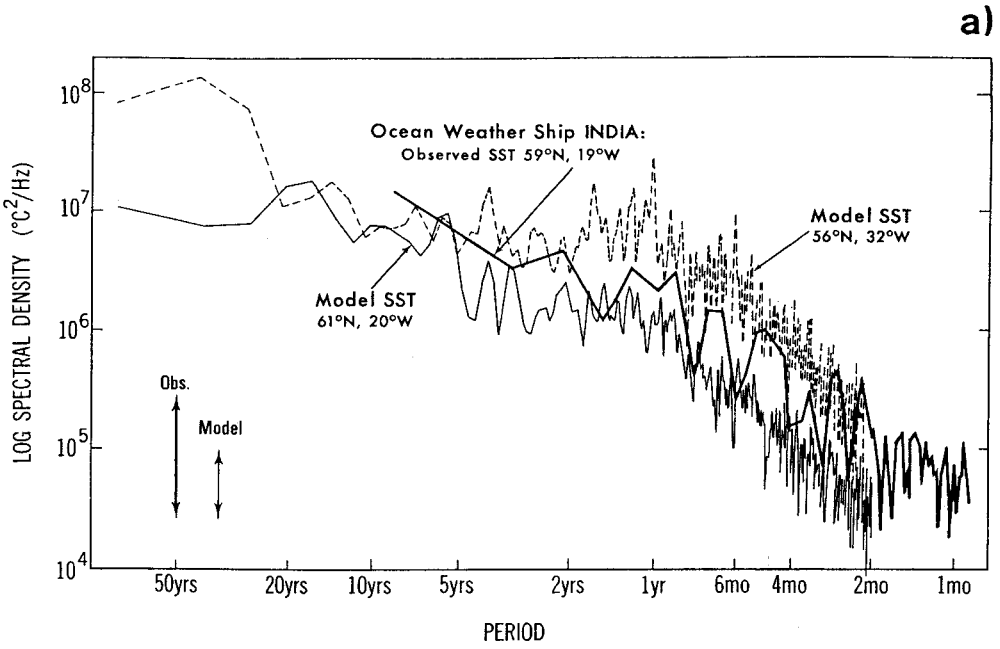
a)
Ocean Weather Ship INDIA:
Observed SST 59°N, 19°W
Model SST
56°N, 32°W
Model SST
61°N, 20°W
Obs.
Model
LOG SPECTRAL DENSITY (°C²/Hz)
PERIOD
50yrs
20yrs
10yrs
5yrs
2yrs
1yr
6mo
4mo
2mo
1mo

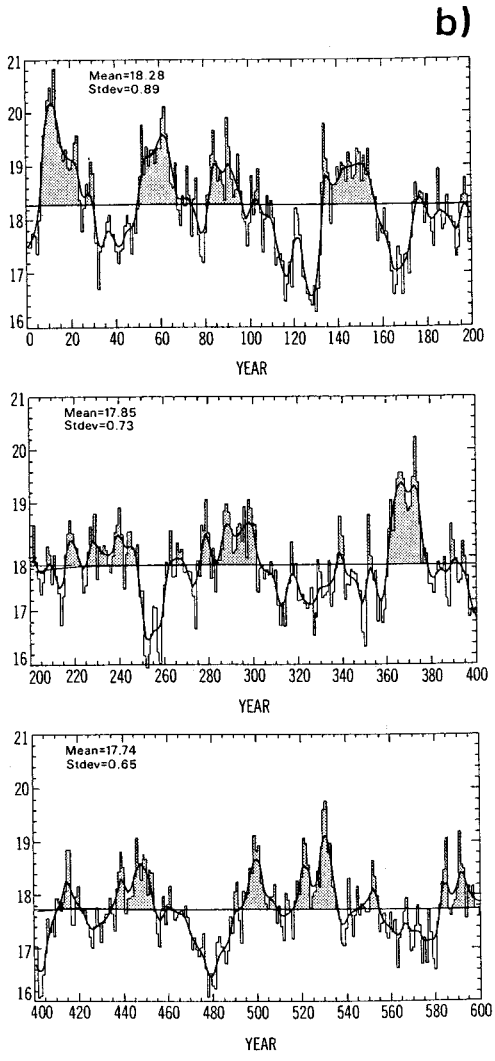
b)
Mean=18.28
Stdev=0.89
Mean=17.85
Stdev=0.73
Mean=17.74
Stdev=0.65
YEAR

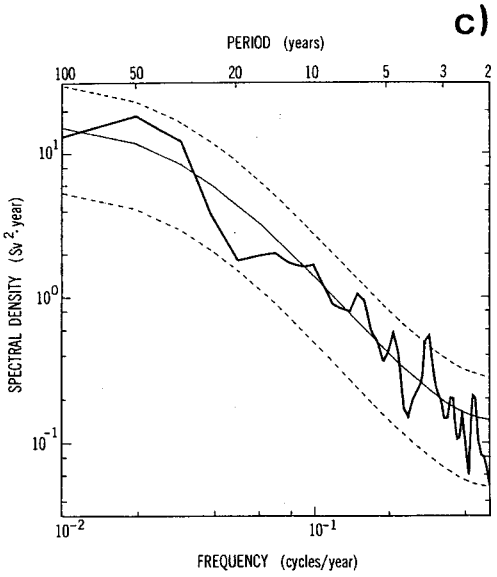
c)
PERIOD (years)
SPECTRAL DENSITY (Sv².year)
FREQUENCY (cycles/year)

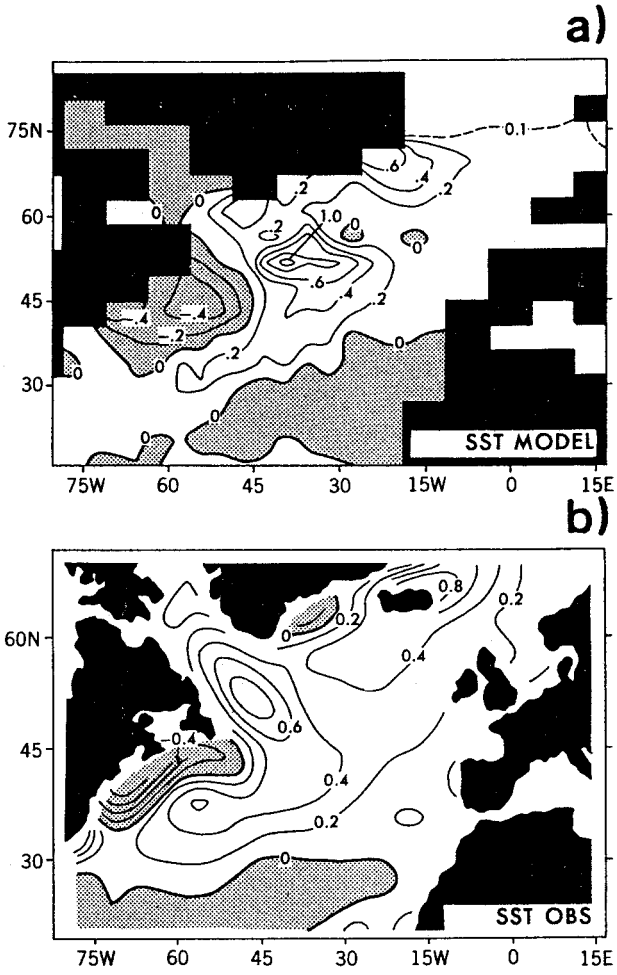

FIG. 17. Comparison of interdecadal North Atlantic SST anomalies (°C) as (a) simulated by Delworth et al. (1993) and (b) derived from observations by subtracting the periods 1950–64 (warm) and 1970–84 (cold) from each other by Kushnir (1994). See Delworth et al. (1993) for details.

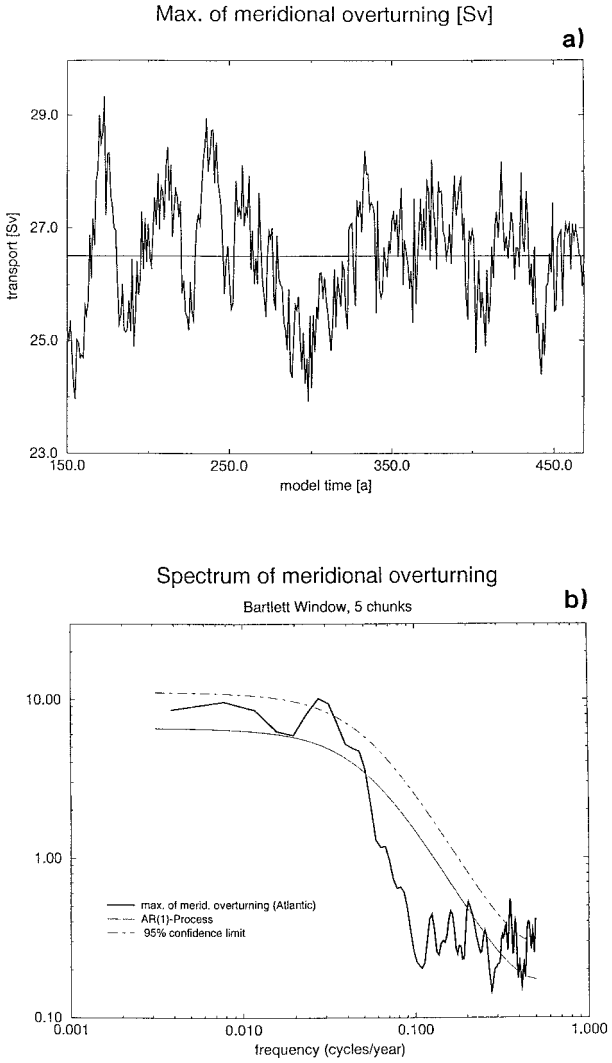

FIG. 18. (a) Time series of an overturning index (Sv) describing the strength of the thermohaline circulation in the experiment with the ECHAM3/LSG CGCM. The overturning index is defined in the same way as in Delworth et al. (1993). (b) Spectrum of the overturning index ($Sv^2 \times a$) shown in (a). See Timmermann et al. (1998) for details.

lationship to the observed SST anomalies in the central North Pacific (Fig. 21), with the anomalous heat content leading the anomalous SST by several years. This suggests that decadal North Pacific SST anomalies are predictable several years ahead. In particular, the strong decadal SST change in the mid-1970s was preceded by a corresponding decadal change in upper-ocean heat content about 5 yr earlier. This feature was also noticed by Zhang and Levitus (1997), who investigated observed surface and subsurface temperature observations (see Figs. 9 and 10).

Griffies and Bryan (1997) investigated the predictability of the Delworth et al. (1993) mode described above by conducting ensembles of classic predictability experiments with the GFDL (coarse-resolution) CGCM. Those were performed in such a way that the coupled model was restarted from initial states obtained from a control integration but with atmospheric perturbations superimposed. The divergences of the trajectories within the forecast ensembles provide information on the pre-

←

FIG. 16. Interdecadal variability as simulated by the GFDL (coarse resolution) CGCM in the North Atlantic. (a) Spectra of two model SST indexes and one observed SST index (the locations are given in the figure). (b) Time series of an overturning index (Sv) describing the strength of the model's thermohaline circulation. (c) Spectrum of the first 200 yr of the overturning index shown in (b). See Delworth et al. (1993) for details.

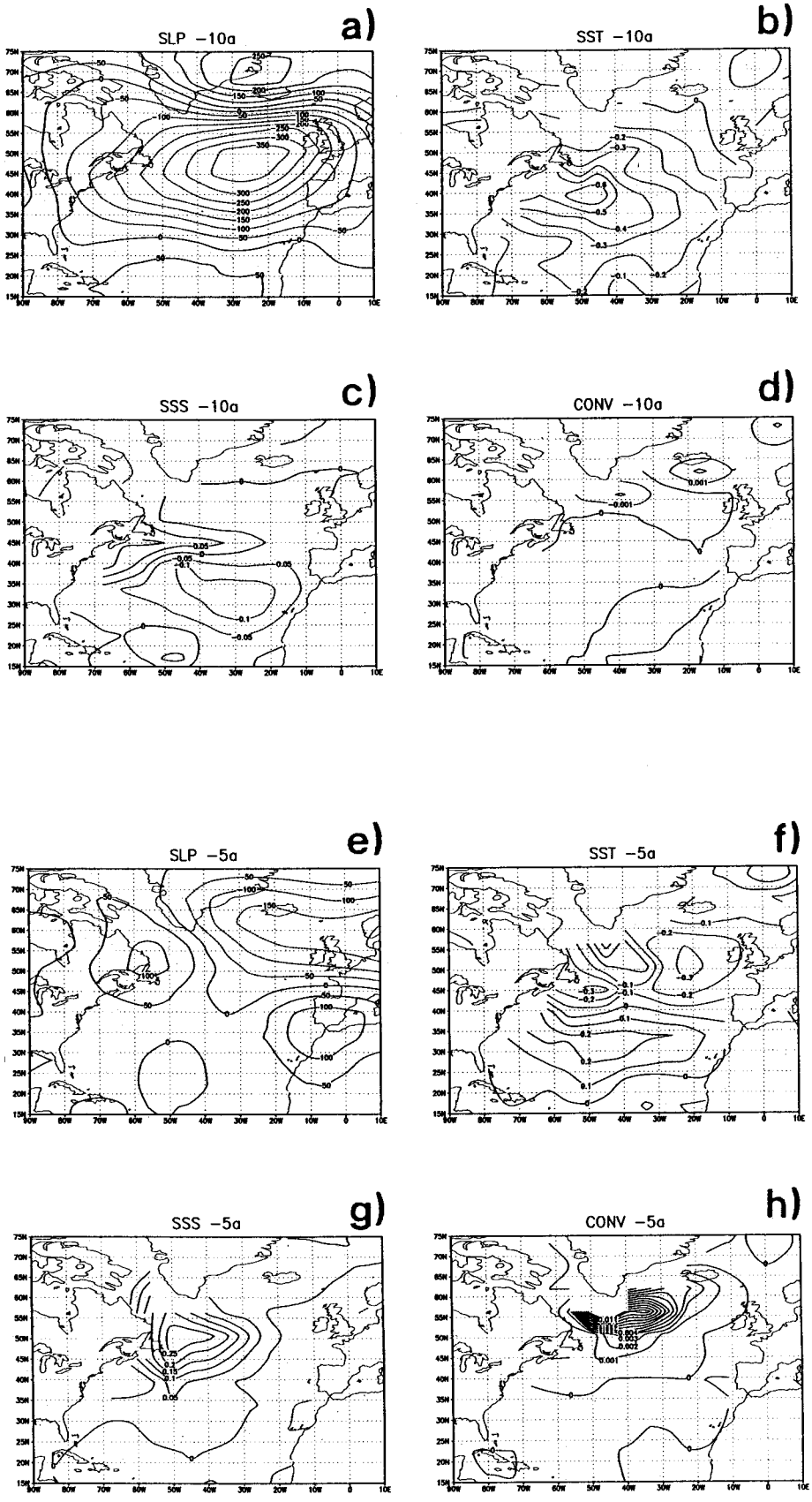
a)
SLP −10a
b)
SST −10a
c)
SSS −10a
d)
CONV −10a
e)
SLP −5a
f)
SST −5a
g)
SSS −5a
h)
CONV −5a

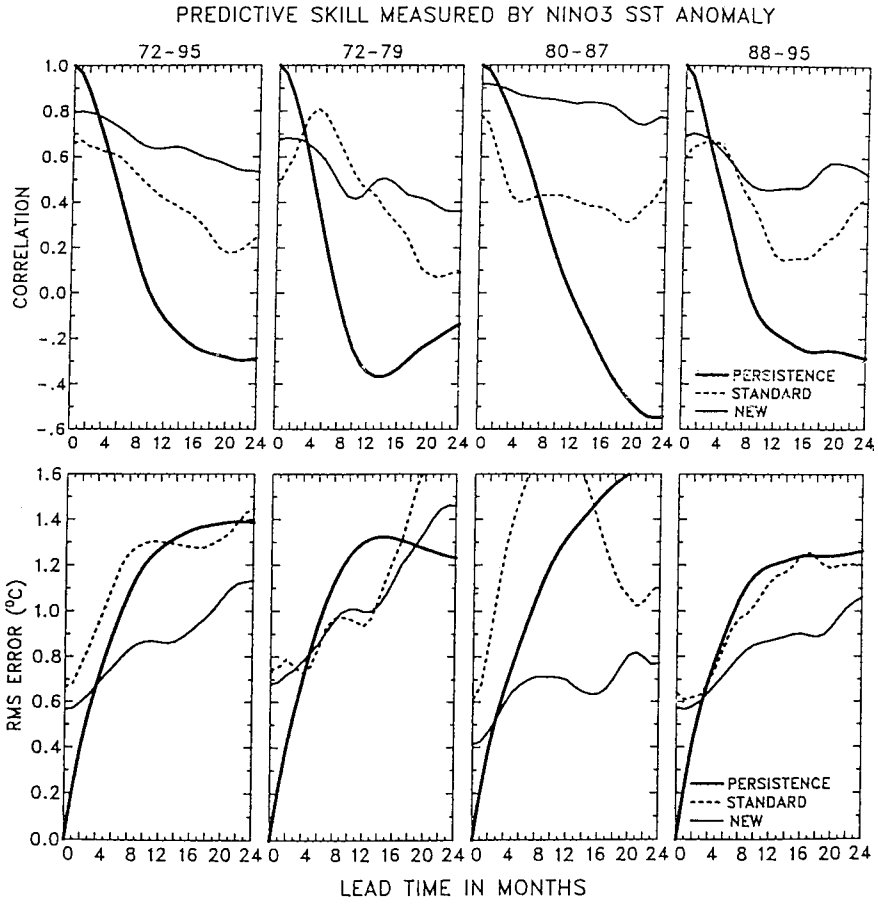

FIG. 20. Correlation skills and rms errors (°C) obtained in predicting eastern equatorial Pacific SST anomalies in the Niño-3 region with two versions of the coupled model of Zebiak and Cane (1987). Shown are the correlation skills and rms errors for different time periods. The top panels show the correlation skills, while the bottom panels show the rms errors. Please note the marked variations in skill from decade to decade. See Chen et al. (1997) for details.

dictability of the coupled system. Griffies and Bryan (1997) derived basically an upper limit of predictability, since they assumed perfect oceanic initial conditions.

Their results indicate that the state of the interdecadal mode described by T. Delworth et al. (1993) as measured by subsurface quantities is predictable up to lead times of one to two decades (Fig. 22). The SST fluctuations associated with the decadal mode, however, appear to be predictable up to lead times of a few years only. The Delworth et al. (1993) mode seems to be connected also to the Arctic climate system, and air–sea interactions may be important in this region (Delworth et al. 1997). This has important consequences for the predictability of SST anomalies in the Greenland Sea, which appear to be predictable about 5–10 yr in advance (T. Delworth 1996, personal communication).

Similar decadal predictability experiments are currently conducted with the ECHAM3/LSG CGCM at MPI (A. Grötzner 1997, personal communication) in order to study the predictability of the interdecadal mode described by Timmermann et al. (1998).

The Delworth et al. (1993) and Timmermann et al. (1998) interdecadal modes appear to have quite different characteristics. While the former can be described to first order as an ocean-only mode, the latter depends crucially on the air–sea coupling. It will be interesting to investigate how this difference manifests itself in the predictabilities of the two modes.

←

FIG. 19. Composites describing the anomalous conditions in different quantities at two different stages of the interdecadal mode simulated by the ECHAM3/LSG CGCM. Panels (a)–(d) show the anomalies 10 yr prior to the maximum overturning. Panels (e)–(h) show the anomalies 5 yr prior to the maximum overturning. The quantities shown are anomalous SLP (Pa), SST (°C), SSS (psu), and potential energy loss by convection (W m^{-2}). See Timmermann et al. (1998) for details.

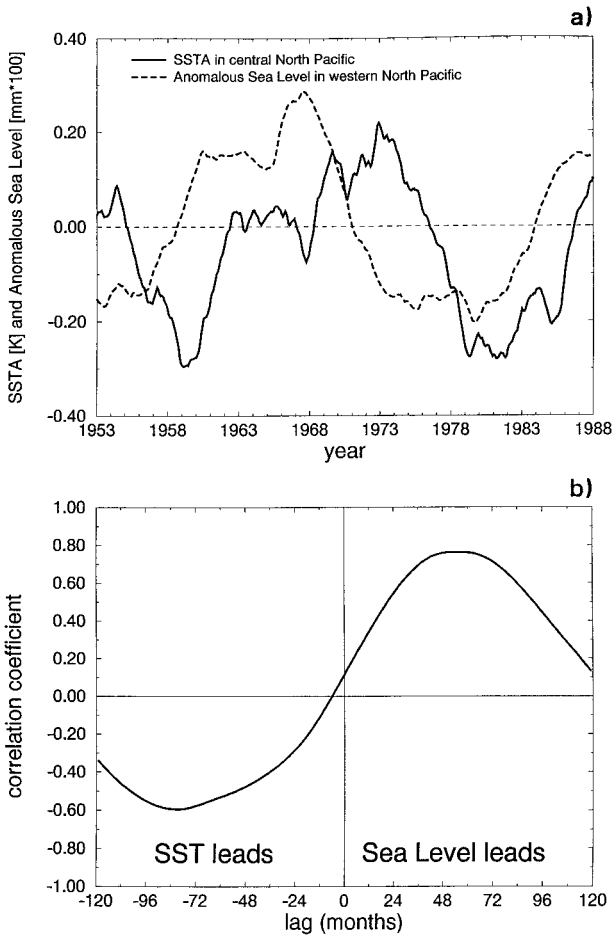

FIG. 21. (a) Time series of anomalous sea level in the western North Pacific as simulated by an oceanic GCM and of observed anomalous SST in the central North Pacific. (b) Lagged cross correlations between the anomalous western Pacific sea level and the anomalous central Pacific SST. Both time series were smoothed by applying a 5-yr running mean filter. Figure provided by S. Venzke.

Ensembles of uncoupled AGCM experiments prescribing observed SSTs and sea ice distributions for several decades are currently performed at different institutions worldwide, in order to study the predictability of the atmosphere at decadal timescales. An example from the Hadley Centre AGCM is described here (Rowell and Zwiers 1997). A six-member ensemble of integrations was conducted for the period October 1948 to December 1993, each experiment starting from different initial conditions. Rowell and Zwiers (1997) found that the Tropics are generally more predictable than the extratropics. The extratropics appear predictable during particular seasons and in particular regions only. Climate anomalies over North America and central Europe, for instance, appear to be predictable in summer but not in winter. Some of these results, however, will be model dependent, and many more such experiments are needed, in order to gain further insight into the nature of the atmospheric response to interdecadal variations in the boundary conditions.

7. Discussion

Coupled ocean–atmosphere models simulate a wide range of interdecadal variability, and many aspects of the simulations show an encouraging similarity with the interdecadal variability observed. Different competing hypotheses, however, were put forward to explain the interdecadal variability in the simulations. Some models, for instance, are largely consistent with Hasselmann's (1976) stochastic climate model scenario, exhibiting relatively featureless red spectra in some oceanographic key quantities. Other models simulate interdecadal oscillations, with statistically significant spectral peaks superimposed on the red background.

One major problem in verifying the different mechanisms proposed is certainly the lack of an adequate observational database, which inhibits us from verifying rigorously the different hypotheses for the generation of interdecadal variability. Reliable surface observations over the oceans exist for approximately the last 100 yr, while reliable land observations may exist for the last 150 yr. High quality subsurface measurements exist for the last few decades only. Thus, there is a strong need to make more use of paleoclimatic data, in order to enhance our understanding of the interdecadal variability. However, it should be possible within the CLIVAR (Climate Variability and Predictability) period to make good progress in the understanding of the short-term decadal variability that occurs on timescales of about 10 yr by an integrated analysis of all available datasets (including paleo-observations, direct observations, and model results) and the collection of new observations.

The role of large-scale air–sea interactions in causing interdecadal variability must be addressed in more detail. One key factor determining the nature of the simulated interdecadal variability, for instance, appears to be the atmospheric response to midlatitudinal SST anomalies. Some atmosphere models seem to be relatively insensitive, while other atmosphere models exhibit a detectable response to extratropical SST anomalies. We are at a relatively early stage in the understanding of the dynamics of this atmospheric response, and further numerical experimentation with state-of-the-art AGCMs will help to advance our understanding. Similarly, the oceanic adjustment in response to changes in the fluxes at the air–sea interface, especially the freshwater flux, is not well understood yet. In particular, it is not clear how well the coarse-resolution OGCMs (which are commonly used in coupled ocean–atmosphere models) simulate the ''real'' ocean.

There are, however, many other problems that need to be addressed in the modeling community, such as the role of flux corrections or the relative importance of salinity and temperature anomalies in the generation of interde-

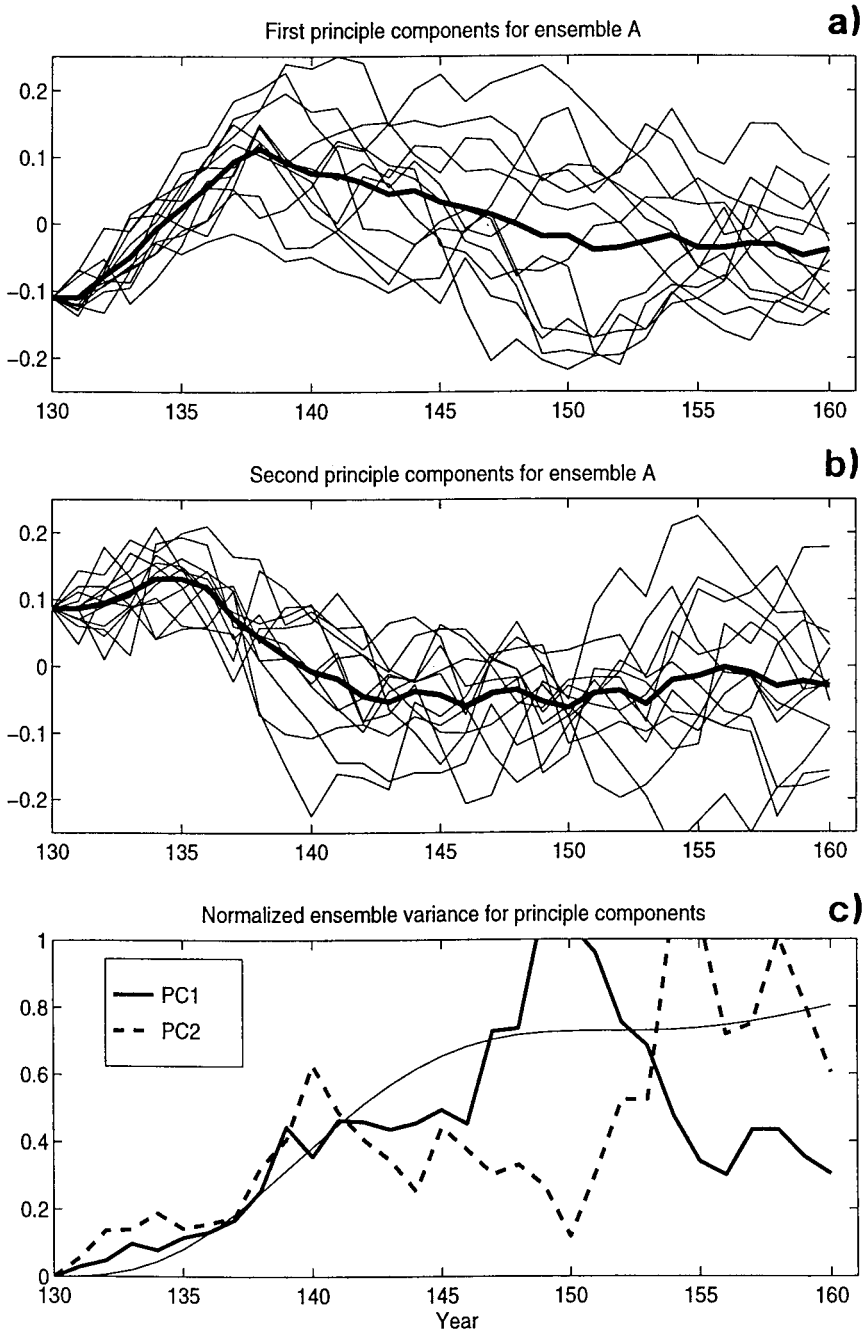

FIG. 22. Results of the predictability experiments conducted by Griffies and Bryan (1997). The top two panels [(a) and (b)] show the evolutions of the first two leading EOFs of dynamic topography, which describe basically the Delworth et al. (1993) mode. The thick lines denote the ensemble means, while the thin lines denote the individual realizations. The normalized ensemble variances are given in (c). See Griffies and Bryan (1997) for details.

cadal variability. Likewise, the relative roles of the Tropics and the extratropics, of stochastic and deterministic processes need to be investigated in more detail. Furthermore, the dependence of the results on model parameterizations and parameters has not yet been adequately explored. The problem of decadal predictability has been addressed so far in very few studies only, and a coordinated international decadal prediction programme under the auspices of CLIVAR would be desirable.

It is likely that the interdecadal variability has some impact on the interannual variability on the one hand, but that the interdecadal variability itself is influenced by cen-

tennial variability and global warming on the other hand. The nature of these interactions are largely unexplored, and much more work is needed during the CLIVAR program to reach a better understanding of these interactions. The anomalous 1990s in the tropical Pacific, for instance, which were characterized by persistent warm conditions and a weak ENSO activity, may be a good example of how the different timescales interact with each other. Some studies argue that the 1990s are already an expression of global warming (e.g., Trenberth and Hoar 1996), while other studies attribute the anomalous 1990s to interdecadal variability (e.g., Latif et al. 1997a), which affected the statistics of the ENSO cycle (Gu and Philander 1997). The bottom line is that models that are applied to the greenhouse warming problem need to simulate realistically both the interannual and interdecadal variability. This, however, is generally not the case. Thus, coupled model development is still a major issue.

Acknowledgments. The author would like to thank Dr. T. Delworth for his valuable comments on an earlier version of the manuscript. Drs. A. Grötzner, M. Münnich, D. Rowell, and S. Zebiak, and Messrs. C. Eckert, A. Timmermann, and S. Venzke provided important input to this review paper. This work was partly sponsored by the European Union under Grant EV5V-CT94-0538 and the German government under Grant 07VK01/1.

APPENDIX

Abbreviations

AGCM	atmospheric general circulation model
CEOF	complex empirical orthogonal function
CCA	canonical correlation analysis
CGCM	coupled general circulation model
CLIVAR	climate variability and predictability
EBM	energy balance model
ENSO	El Niño/Southern Oscillation
EOF	empirical orthogonal function
GCM	general circulation model
GFDL	Geophysical Fluid Dynamics Laboratory
HCM	hybrid coupled model
ICM	intermediate coupled model
ITCZ	intertropical convergence zone
MPI	Max-Planck-Institut für Meteorologie
NAO	North Atlantic Oscillation
OGCM	oceanic general circulation model
PNA	Pacific–North American pattern
SLP	sea level pressure
SSS	sea surface salinity
SST	sea surface temperature

REFERENCES

Anderson, D. L. T., and J. Willebrand, 1996: *Decadal Climate Variability: Dynamics and Predictability*. Vol. 44, *Global Environmental Change*, NATO ASI Series, Springer, 493 pp.

Balmaseda, M. A., M. K. Davey, and D. L. T. Anderson, 1995: Decadal and seasonal dependence of ENSO prediction skill. *J. Climate*, **8,** 2705–2715.

Barnett, T. P., M. Latif, N. Graham, M. Flügel, S. Pazan, and W. B. White, 1993: ENSO and ENSO-related predictability. Part I: Prediction of equatorial Pacific sea surface temperature with a hybrid coupled ocean–atmosphere model. *J. Climate,* **6,** 1545–1566.

Bjerknes, J., 1964: Atlantic air–sea interaction. *Advances in Geophysics*, Academic Press, Vol. 10, 1–82.

Carton, J. A., and B. Huang, 1994: Warm events in the tropical Atlantic. *J. Phys. Oceanogr.,* **24,** 888–893.

——, X. Cao, B. S. Giese, and A. M. da Silva, 1996: Decadal and interannual SST variability in the tropical Atlantic Ocean. *J. Phys. Oceanogr.,* **26,** 1165–1175.

Chang, P., L. Ji, and H. Li, 1997: A decadal climate variation in the tropical Atlantic Ocean from thermodynamic air–sea interactions. *Nature,* **385**, 516–518.

Chen, D., S. E. Zebiak, M. A. Cane, and A. J. Busalacchi, 1997: On the initialization and predictability of a coupled ENSO forecast model. *Mon. Wea. Rev.,* **125,** 773–788.

Chen, F., and M. Ghil, 1996: Interdecadal variability in a hybrid coupled ocean–atmosphere model. *J. Phys. Oceanogr.,* **26,** 1561–1578.

Cubasch, U., R. Voss, G. C. Hegerl, J. Waskewitz, and T. J. Crowley, 1997: Simulation of the influence of solar radiation variations on the global climate with an ocean–atmosphere general circulation model. *Climate Dyn.* **13**, 757–767.

da Silva, A. M., C. C. Young, and S. Levitus, 1994: Atlas of surface marine data 1994, Vols. 1 and 3. NOAA Atlas NESDIS 6 and 8, 83 pp. [Available from NOCD, NOAA/NESDIS E/OC21, Washington, DC 20235.]

Delworth, T., 1996: North Atlantic interannual, variability in a coupled ocean–atmosphere model. *J. Climate,* **9,** 2356–2375.

——, S. Manabe, and R. J. Stouffer, 1993: Interdecadal variations of the thermohaline circulation in a coupled ocean–atmosphere model. *J. Climate,* **6,** 1993–2011.

——, ——, and ——, 1997: Multidecadal climate variability in the Greenland Sea and surrounding regions: A coupled model simulation. *Geophys. Res. Lett.,* **24**, 257–260.

Deser, C., and M. L. Blackmon, 1993: Surface climate variations over the North Atlantic Ocean during winter: 1900–1989. *J. Climate*, **6,** 1743–1753.

——, M. A. Alexander, and M. S. Timlin, 1996: Upper-ocean thermal variations in the North Pacific during 1970–91. *J. Climate,* **9,** 1840–1855.

Dickson, R. R., J. Meincke, S.-A. Malmberg, and A. J. Lee, 1988: The ''great salinity anomaly'' in the northern North Atlantic 1968–1982. *Progress in Oceanography*, Vol. 20, Pergamon Press, 103–151.

Eckert, C., and M. Latif, 1997: Predictability of a stochastically forced hybrid coupled model of El Niño. *J. Climate,* **10,** 1488–1504.

Enfield, D. B., and D. A. Mayer, 1997: Tropical Atlantic SST variability and its relationship to El Niño–Southern Oscillation. *J. Geophys. Res.,* **102** (C1), 929–945.

Folland, C. K., T. N. Palmer, and D. E. Parker, 1986: Sahel rainfall and worlwide sea temperatures. *Nature*, **320,** 602–607.

Frankignoul, C., and K. Hasselmann, 1977: Stochastic climate models. Part II: Application to sea surface temperature variability and thermocline variability. *Tellus*, **29,** 284–305.

——, P. Müller, and E. Zorita, 1997: A simple model of the decadal response of the ocean to stochastic wind forcing. *J. Phys. Oceanogr.,* **27,** 1533–1546.

Glantz, M. H., R. W. Katz, and N. Nicholls, 1991: *Teleconnections Linking Worldwide Climate Anomalies.* Cambridge University Press, 535 pp.

Goddard, L., and N. E. Graham, 1997: El Niño in the 1990s. *J. Geophys. Res.*, **102**, 10 423–10 436.

Griffies, S. M., and E. Tziperman, 1995: A linear thermohaline oscillator driven by stochastic atmospheric forcing. *J. Climate,* **8,** 2440–2453.

——, and K. Bryan, 1997: Ensemble predictability of simulated North Atlantic interdecadal climate variability. *Science,* **275,** 181–184.
Grötzner, A., M. Latif, and T. P. Barnett, 1998: A decadal climate cycle in the North Atlantic Ocean as simulated by the ECHO coupled GCM. *J. Climate,* in press.
Gu, D., and S. G. H. Philander, 1997: Interdecadal climate fluctuations that depend on exchanges between the Tropics and extratropics. *Science,* **275,** 805–807.
Hasselmann, K., 1976: Stochastic climate models. Part I: Theory. *Tellus,* **28,** 473–485.
Haston, L., and J. Michaelson, 1994: Long-term central coastal California precipitation variability and relationships to El Niño. *J. Climate,* **7,** 1373–1387.
Horel, J. D., and J. M. Wallace, 1981: Planetary-scale atmospheric phenomena associated with the Southern Oscillation. *Mon. Wea. Rev.,* **109,** 813–829.
Houghton, R. W., and Y. M. Tourre, 1992: Characteristics of low-frequency sea surface temperature fluctuations in the tropical Atlantic. *J. Climate,* **5,** 765–771.
Jacobs, G. A., H. E. Hurlbert, J. C. Kindle, E. J. Metzger, J. L. Mitchell, W. J. Teague, and A. J. Wallcraft, 1994: Decade-scale trans-Pacific propagation and warming effects of an El Niño anomaly. *Nature,* **370,** 360–363.
James, I. N., and P. M. James, 1989: Ultra-low-frequency variability in a simple atmospheric model. *Nature,* **342,** 53–55.
Ji, M., A. Leetmaa, and V. E. Kousky, 1996: Coupled model forecasts of ENSO during the 1980s and 1990s at the National Centers for Environmental Prediction. *J. Climate,* **9,** 3105–3120.
Jiang, S., F.-F. Jin, and M. Ghil, 1995: Multiple equilibria, periodic, and aperiodic solutions in a wind-driven, double gyre, shallow-water model. *J. Phys. Oceanogr.,* **25,** 764–786.
Jin, F.-F., J. D. Neelin, and M. Ghil, 1994: El Niño on the devil's staircase: Annual subharmonic steps to chaos. *Science,* **264,** 70–72.
Kushnir, Y., 1994: Interdecadal variations in the North Atlantic sea surafce temperature and associates atmospheric conditions. *J. Climate,* **7,** 141–157.
Labitzke, K., 1987: Sunspots, the QBO, and the stratospheric temperature in the north polar region. *Geophys. Res. Lett.,* **14,** 535–537.
Lamb, P. J., and R. A. Peppler, 1991: Regional case studies of teleconnections: Physical aspects. West Africa. *Teleconnections Linking Worldwide Climate Anomalies,* Cambridge University Press, 121–189.
Latif, M., and T. P. Barnett, 1994: Causes of decadal climate variability over the North Pacific and North America. *Science,* **266,** 634–637.
——, and ——, 1996: Decadal climate variability over the North Pacific and North America: Dynamics and predictability. *J. Climate,* **9,** 2407–2423.
——, T. Stockdale, J. Wolff, G. Burgers, E. Maier-Reimer, and M. M. Junge, 1994: Climatology and variability in the ECHO coupled GCM. *Tellus,* **46A,** 351–366.
——, A. Grötzner, and H. Frey, 1996a: El Hermanito: El Niño's overlooked little brother in the Atlantic. Max-Planck-Institut für Meteorologie Rep. 196, 14 pp. [Available from Max-Planck-Institut für Meteorologie, Bundesstrasse 55, D-20146 Hamburg, Germany.]
——, ——, M. Münnich, E. Maier-Reimer, S. Venzke, and T. P. Barnett, 1996b: A mechanism for decadal climate variability. *Decadal Climate Variability: Dynamics and Predictability,* Vol. 44, *Global Environmental Change,* NATO ASI Series, Springer, 263–292.
——, R. Kleeman, and C. Eckert, 1997a: Greenhouse warming, decadal variability, or El Niño? An attempt to understand the anomalous 1990s. *J. Climate,* **10,** 2221–2239.
——, A. Grötzner, A. Timmermann, S. Venzke, and T. P. Barnett, 1997b: Dynamics of decadal climate variability over the Northern Hemisphere. *Proc. JCESS/CLIVAR Workshop on Decadal Climate Variability,* Columbia MD, Max-Planck-Institut für Meteorologie, Appendix A.
——, and Coauthors, 1998: TOGA review paper: Predictability and Prediction. *J. Geophys. Res.,* in press.
Lean, J., J. Beer, and R. Bradley, 1995: Reconstruction of solar irradiance since 1600: Implications for climate change. *Geophys. Res. Lett.,* **22,** 3195–3198.
Levitus, S., and J. Antonov, 1995: Observational evidence of interannual to decadal-scale variability of the subsurface temperature-salinity structure of the World Ocean. *Climate Change,* Kluwer Academic, 495–514.
——, T. P. Boyer, and J. Antonov, 1994: *World Ocean Atlas 1994.* Vol. 5, *Interannual Variability of Upper Ocean Thermal Structure,* U.S. Department of Commerce, NOAA, 176 pp.
Liu, Z., and S. G. H. Philander, 1995: How different wind stress patterns affect the tropical subtropical circulations of the upper ocean. *J. Phys. Oceanogr.,* **25,** 449–462.
——, ——, and R. C. Pacanowski, 1994: A GCM study of the tropical–subtropical upper-ocean water exchange. *J. Phys. Oceanogr.,* **24,** 2606–2623.
Lohmann, G., 1996: Stability of the thermohaline circulation in analytical and numerical models. Ph.D. thesis, University of Bremen. [Available from Alfred-Wegener-Institut für Polar- und Meeresforschung, D-27568 Bremerhaven, Germany.]
Lu, P., and J. P. McCreary, 1995: Influence of the ITCZ on the flow of thermocline water from the subtropical to the equatorial Pacific Ocean. *J. Phys. Oceanogr.,* **25,** 3076–3088.
Manabe, S., and R. J. Stouffer, 1996: Low-frequency variability of surface air-temperature in a 1000-yr integration of a coupled atmosphere–ocean–land surface model. *J. Climate,* **9,** 376–393.
Mann, M. E., and J. Park, 1994: Global-scale modes of surface temperature variability on interannual to century timescales. *J. Geophys. Res.,* **99,** 25 819–25 833.
Mantua, N. J., S. R. Hare, Y. Zhang, J. M. Wallace, and R. C. Francis, 1997: A Pacific interdecadal climate oscillation with impacts on salmon production. *Bull. Amer. Meteor. Soc.,* **78,** 1069–1080.
Meehl, G. A., 1996: Characteristics of decadal variability in a global coupled GCM. *Proc. JCESS/CLIVAR Workshop on Decadal Climate Variability,* Columbia, MD, Max-Planck-Institut für Meteorologie, Appendix A.
Mehta, V. M., 1998: Variability of the tropical ocean surface temperatures at decadal-multidecadal timescales. Part I: The Atlantic Ocean. *J. Climate,* in press.
——, and T. Delworth, 1995: Decadal variability of the tropical Atlantic ocean surface temperature in shipboard measurements and in a global ocean–atmosphere model. *J. Climate,* **8,** 172–190.
Mikolajewicz, U., and E. Maier-Reimer, 1990: Internal secular variability in an ocean general circulation model. *Climate Dyn.,* **4,** 145–156.
Moura, A. D., and J. Shukla, 1981: On the dynamics of drought in northeast Brazil: Observations, theory, and numerical experiments with a general circulation model. *J. Atmos. Sci.,* **38,** 2653–2675.
Münnich, M., M. A. Cane, and S. E. Zebiak, 1991: A study of self-excited oscillations in a tropical ocean–atmosphere system. Part II: Nonlinear cases. *J. Atmos. Sci.,* **48,** 1238–1248.
Mysak, L. A., D. K. Manak, and R. F. Mardsen, 1990: Sea-ice anomalies in the Greenland and Labrador Seas 1900–84 and their relation to an interdecadal Arctic climate cycle. *Climate Dyn.,* **5,** 111–133.
Neelin, J. D., M. Latif, and F.-F. Jin, 1994: Dynamics of coupled ocean–atmosphere models: The tropical problem. *Annu. Rev. Fluid Mech.,* **26,** 617–659.
Palmer, T. N., and Z. Sun, 1985: A modelling and observational study of the relationship between sea surface temperature in the northwest Atlantic and the atmospheric general circulation. *Quart. J. Roy. Meteor. Soc.,* **111,** 947–975.
Philander, S. G. H., 1990: *El Niño, La Niña, and the Southern Oscillation.* Academic Press, 293 pp.
Robertson, A. W., 1996: Interdecadal variability over the North Pa-

cific in a multi-century climate simulation. *Climate Dyn.,* **12,** 227–241.
Robock, A. D., and J. Mao, 1995: The volcanic signal in surface temperature observations. *J. Climate,* **8,** 1086–1103.
Rowell, D. P., and F. W. Zwiers, 1997: Sources of atmospheric decadal variability. *Proc. 7th Conf. on Climate Variations,* Long Beach, CA, Amer. Meteor. Soc., 87–89.
Saravanan, R., and J. C. McWilliams, 1997: Stochasticity and spatial resonance in interdecadal climate fluctuations. *J. Climate,* **10,** 2299–2320.
Spall, M. A., 1996: Dynamics of the Gulf Stream/deep western boundary current crossover. Part II: Low-frequency internal oscillations. *J. Phys. Oceanogr.,* **26,** 2169–2182.
Tett, S. F. B., T. C. Johns, and J. F. B. Mitchell, 1998: Global and regional variability in a coupled AOGCM. *Climate Dyn.,* in press.
Timmermann, A., M. Latif, R. Voss, and A. Grötzner, 1998: Northern Hemispheric interdecadal variability: A coupled air–sea mode. *J. Climate,* in press.
Trenberth, K. E., and J. W. Hurrell, 1994: Decadal atmosphere–ocean variations in the Pacific. *Climate Dyn.,* **9,** 303–319.
——, and T. J. Hoar, 1996: The 1990–95 El Niño–Southern Oscillation event: Longest on record. *Geophys. Res. Lett.,* **23,** 57–60.
von Storch, J.-S., 1994: Interdecadal variability in a global coupled model. *Tellus,* **46A,** 419–432.
Weaver, A. J., and E. S. Sarachik, 1991: Evidence for decadal variability in an ocean general circulation model: An advective mechanism. *Atmos.–Ocean,* **29,** 197–231.
——, J. Marotzke, P. F. Cummins, and E. S. Sarachik, 1993: Stability and variability of the thermohaline circulation. *J. Phys. Oceanogr.,* **23,** 39–60.
Weisse, R., U. Mikolajewicz, and E. Maier-Reimer, 1994: Decadal variability of the North Atlantic in an ocean general circulation model. *J. Geophys. Res.,* **99,** 12 411–12 421.
Wohlleben, T. M. H., and A. J. Weaver, 1995: Interdecadal variability in the subpolar North Atlantic. *Climate Dyn.,* **11,** 459–467.
Xu, W., T. P. Barnett, and M. Latif, 1998: Decadal variability in the North Pacific as simulated by a hybrid coupled model. *J. Climate,* **11,** 297–312.
Zebiak, S. E., 1993: Air–sea interaction in the equatorial Atlantic region. *J. Climate,* **6,** 1567–1586.
——, and M. A. Cane, 1987: A model El Niño/Southern Oscillation. *Mon. Wea. Rev.,* **115,** 2262–2278.
Zhang, R.-H., and S. Levitus, 1997: Structure and cycle of decadal variability of upper ocean temperature in the North Pacific. *J. Climate,* **10,** 710–727.
——, J. M. Wallace, and D. S. Battisti, 1997: ENSO-like interdecadal variability: 1900–93. *J. Climate,* **10,** 1004–1020.
Zorita, E., and C. Frankignoul, 1997: Modes of North Atlantic decadal variability in the ECHAM1/LSG coupled ocean–atmosphere general circulation model. *J. Climate,* **10,** 183–200.